XYLAN DEPOSITION ON THE SECONDARY WALL OF THE FAGUS CRENATA FIBER

2002

TATSUYA AWANO

XYLAN DEPOSITION ON THE SECONDARY WALL OF THE FAGUS CRENATA FIBER

2002

TATSUYA AWANO

Preface

The author wishes to express his sincere thanks to **Professor Minoru Fujita**, Division of Forest and Biomaterials Science, Graduate School of Agriculture, Kyoto University, for his kind guidance and encouragement during the course of this study.

The author also wishes to express his thanks to **Professor Jun' ichi Azuma**, Division of Environmental Science and Technology, Graduate School of Agriculture, Kyoto University, and **Professor Takao Itoh**, Wood Research Institute, Kyoto University, for their valuable suggestions and critical readings of the manuscript.

The author wishes to express special thanks to **Associate Professor Keiji Takabe**, Division of Forest and Biomaterials Science, Graduate School of Agriculture, Kyoto University, for his kind valuable suggestions for this entire work and encouragement.

The author greatly appreciates to **Associate Professor Noboru Manabe**, Division of Applied Biosciences, Graduate School of Agriculture, Kyoto University and **Dr. Miki Sugimoto**, Applied Biosciences, Graduate School of Agricultural, Kyoto University, for their kind help in dealing with mice and their valuable suggestions on antibody production.

The author also greatly appreciates to **Associate Professor Takashi Watanabe**, Wood Research Institute, Kyoto University, and **Associate Professor Takahisa Hayashi**, Wood Research Institute, Kyoto University, for kindly providing xylan and xyloglucan and valuable information on these molecules.

The author wishes to express his special thanks to **Professor Geoffrey Daniel**, Wood Ultrastructure Research Centre, Swedish University of Agricultural Sciences, for our collaboration in immuno FESEM study and his hospitality in Uppsala.

The author is deeply grateful to **Dr. Takahiko Higasa**, Research Institute for Food Science, Kyoto University, for teaching FESEM overation and useful discussion on FESEM images.

Special thanks are also due to **Professor Iwao Furusasa**, Division of Applied

Biosciences, Graduate School of Agriculture, Kyoto University, and **Associate Professor Kazuyuki Mise**, Division of Applied Biosciences, for their valuable suggestions on the enzyme immuno assay.

The author wishes to express his thanks to **Professor Kunisuke Tanaka**, Kyoto Prefectural University, **Associate Professor Takehiro Masumura**, Kyoto Prefectural University, and **Dr. Sigeto Morita**, Kyoto Prefectural University, for their valuable helps and advice.

Finally, the author wishes to express his thanks to **Emeritus Professor Hiroshi Saiki**, Kyoto University, **Dr. Arata Yoshinaga**, Division of Forest and Biomaterials Science, Graduate School of Agriculture, Kyoto University, and **other members** of Laboratory of Plant Cell Structure, Division of Forest and Biomaterials Science, Graduate School of Agriculture, Kyoto University, for their valuable discussions and assistance during the course of this study.

January 28, 2002

Tatsuya Awano

Tatsuya Awano

Contents

Chapter 1

Introduction

1.1 Molecular properties of xylan

Hemicelluloses are the second most abundant materials following cellulose in hardwoods. Xylan, in particular, accounts for 20 to 30% of cell wall materials of hardwoods (Fengel and Wegener 1989). The term "xylan" is a generic name of homopolysaccharide that is composed of a linear backbone of β-(1,4)-linked-D-xylopyranose. Xylans are widely distributed in the land plants. In the case of hardwoods, xylan is irregularly substituted by 4-*O*-methyl-β-D-glucuronic acid with an α-(1,2)-glicoside linkage and many of the OH-groups at C2 and C3 of the xylose unit are substituted by *O*-acetyl groups (Bastawde 1992). Therefore, xylan in hardwoods is formally called *O*-acetyl-4-*O*-methylglucuronoxylan. Most of the xylan isolated from various hardwoods have a side chain of 4-*O*-methylglucuronic acid per ten xylose units.

The chemical properties of xylan were reviewed and their possible role were postulated by many authors. Xylan can tightly bind to cellulose microfibrils because of the hydrogen-bondings between the xylose backbone and the glucan chain of cellulose microfibrils (Labavitch and Ray 1974; McNeil et al. 1975; Mora et al. 1986; Neville 1988; Brett et al. 1997). Xylan gives negative charges onto the surface of cellulose microfibrils owing to their 4-*O*-metyl-glucuronic acid groups. This separates each cellulose microfibril and enables them to assemble in helicoidal structure *in vitro* (Vian et al. 1994) and *in vivo* (Vian et al. 1986, 1992; Reis et al. 1992). Another role of xylan is as a host structure for lignin precursors. Taylor and Haigler (1993) suggested that the secondary wall assembly occurs as a self-perpetuating cascade in which xylan mediate the localization of lignin.

1.2 Distribution of xylan

The chemical composition of cell wall layers has not been determined precisely because cell walls could not be divided into their cell wall layers. Meier and Wilkie

(1959) and Meier (1961) divided the radial sections of differentiating tissue into four different fractions with the aid of a polarized microscope and a micromanipulator; the first fraction consisting of cells with middle lamella and primary wall (M+P), the second containing the cells with M+P and the outer layer of secondary wall ($M+P+S_1$), the third containing the cells with $M+P+S_1$ and the outer part of secondary wall ($M+P+S_1+S_2$), and finally the complete cells ($M+P+S_1+S_2+S_3$). After acid hydrolysis of these fractions their sugar compositions were quantitatively determined. Thereafter, they calculated the proportion of polysaccharides in each cell wall layer as a difference of these fractions, for example, the proportion of S_1 layer was determined by the difference between ($M+P+S_1$) and (M+P). They suggested that the xylan content in birch fibers increased at first, reaching a maximum in the S_2 forming fibers, and then decreased again in the fully developed fibers. The problem of this method is that the calculation was based on two hypothesis; the density of cell wall layer is the same in each layer, and the proportion of polysaccharide in each layer never changes during cell wall maturation.

Takabe et al. (1983) fractionated a series of tangential sections from the differentiating xylem tissue of *Cryptomeria japonica* into various fractions according to developing stages. Thereafter, they determined the amount of sugars in each fraction by gas-liquid-chromatography. Xylose deposited actively from the latter stage of S_1 to the beginning stage of S_2, and from the final stage of S_2 to the S_3 stage. This result was supported by the tracer experiments using ^{14}C-glucose (Takabe et al. 1981). The proportion of radioactive xylose was high in the early part of S_2 stage and S_3 stage. Based on these findings, they concluded that xylan deposits in the outer part of S_2 layer and also S_3 layer. The estimation, however, was based on the hypothesis that xylan deposits to the inner surface of the cell wall without penetration.

In the early 80's, ultrastructural cytochemistry by the subtraction combining mild chemical or enzymatic extractions coupled with cytochemical staining has largely

contributed to reveal the polysaccharides distribution in various types of primary wall and secondary wall (Prameswaran and Sinner 1979; Prameswaran and Liese 1982; Roland and Mosiniak 1982; Vian 1982; Catesson 1983; Catesson et al. 1994). However, these methods based on structural changes after extraction and therefore did not lead to a direct visualization of polysaccharides.

Direct visualization of molecular distribution is achieved by affinity labeling method, which contains enzyme-gold labeling method and immuno-gold labeling method. The first attempt to label xylan distribution was xylanase-gold labeling. Vian et al. (1983) prepared a complex of xylanase and colloidal gold which allows the direct visualization of xylan distribution under a transmission electron microscope. Xylanase is the enzyme that specifically binds to β-1,4-xylan and depolymerizes them, however, in resin-embedded specimen a strong and stable binding is likely to occur between the xylanase-gold and the substrate (xylan) without depolymerization (Vian et al. 1983). The xylanase-gold probe was highly specific for β-1,4-xylopyranosyl linkages which is confirmed by various substrates such as xylan, polygalacturonic acid, arabinans, galactans, avicel and carboxymethylcellulose. Vian et al. (1986, 1992) examined the xylan distribution in linden wood by the xylanase-gold labeling. They found that xylan distributed in the S_1 - S_2 transition zone of fiber secondary wall where microfibrils have a helicoidal alignment, i.e. progressively change their microfibril angle from large to small. From these findings, they hypothesized that xylan may act as a twisting agent for cellulose microfibrils.

The immunogold labelling is one of the most powerful methods to visualize the localization of particular molecules when the antibody is specific to the targeted molecule. Northcote et al. (1989) prepared anti-β-xylo-oligosaccharide antiserum and revealed that xylan localized in the secondary wall thickening of mesopyll cells of cultures of *Zinnia elegans*. Migné et al. (1994) produced two types of antibodies, one against oat arabinoxylan which contained 10% arabinose and another against 4-*O*-methyl-glucuronoxylan. Labeling for both antibodies was detected in the cell walls of

sclerenchyma, parenchyma, xylem and lignified fibers at various developmental stages of maize internode indicating that the distribution of both xylans were same at the tissue level. Particularly, the secondary wall showed intense labeling with both antibodies. Suzuki et al. (2000) prepared two types of antisera which recognized highly substituted glucuronoarabinoxylan (hsGAXs) and low-branched xylan. They demonstrated that these antisera did not cross-react with each other. Thereafter, they observed the localization of xylans in maize tissue and proposed that hsGAX and low-branched xylan have separate functions in lignified and unlignified tissues, because the former is localized mainly in unlignified walls, though the latter in lignified walls.

1.3 Ultrastructure of the wood cell wall

Multilayered structure of wood cell wall was revealed by transmission electron microscopy in early studies (Harada 1965). Sub-layer structure, i.e. alignment of fibrils and spatial relationship between fibrils and matrix components, were investigated by various techniques, such as ultrathin-sectioning followed by positive or negative staining (Kerr and Goring 1975; Ruel et al. 1978; Donaldson and Singh 1998), conventional surface replication (Kataoka et al. 1992), surface replication coupled with rapid-freeze deep-etching (RFDE) (Fujino and Itoh 1998; Hafrén et al. 1999), and field emission scanning electron microscopy (Abe et al. 1991,1992; Sell and Zimmermann 1993a, 1993b). In these investigations, fibrous components are embedded in matrix components. The fibrils are thought to represent the assembly of cellulose molecules with ordered and less ordered regions. Cellulose fibrils with a diameter ranging from 10 to 25 nm are called 'microfibrils' (Frey-Wyssling 1954). Although microfibril was assumed to be the smallest unit in early studies, smaller units with an average diameter of 3.5 nm, called 'elementally fibril', were detected later (Mühlethaler 1965, Heyn 1966, 1969). A larger fibril component with a diameter of 30 to 100 nm is called 'macrofibril' or 'fibril

agglomeration' (Sell and Zimmermann 1993a). Delmer and Amor (1995) defined the term 'microfibril' as follows: Microfibril is composed of 36 glucose chains in the primary wall of plants, and during the synthesis of secondary wall, microfibrils often associate further to form bundles or macrofibrils.

A model taking into account the presence of lignin and hemicellulose was proposed by Fengel (1970), Kerr and Goring (1975) and Donaldson and Singh (1998) . In the Fengel model, smallest units of cellulose fibrils (3 nm) are separated from each other by monomolecular layer of hemicellulose, and they form microfibrils 12 nm in width. The largest units (25 nm in diameter), which is composed of some microfibrils, are surrounded by hemicellulose and lignin. The Kerr and Goring model is well known as 'interrupted lamella' model. Tangential alignment of cellulose microfibrils are interrupted in tangential and radial direction by lignin-hemicellulose matrix. Recently, Donaldson and Singh (1998) proposed a model of the wood cell wall which consists of cellulose fibrils (3.6 nm in diameter) surrounded in a sheath of hemicellulose (1 nm in thickness) and interfibrillar bridges of hemicellulose.

The fibrils observed by field emission scanning electorn microscopy are not necessarily just celluose. In the present thesis, therefore, the terms 'microfibril' and 'macrofibril' are used as follows:

Microfibril -- The smallest fibrilar component of the cell wall observed by electron microscopy. They are long fibrils with 3-4 nm in diameter and consisting of a group of cellulose molecules surrounded by a sheath of hemicelluloses (Donaldson and Singh 1998). The term 'cellulose microfibril' is used specifically for fibrils with 3-4 nm in diameter which are composed of cellulose molecules.

Macrofibril -- A larger fibril component of the secondary wall typically 10-20 nm in diameter as typically observed by field emission scanning electron microscopy and surface replica (Abe et al. 1991, 1992; Fujino and Itoh 1998; Hafrén et al. 1999). Macrofibrils are composed of a group of microfibrils and are coated with

other cell wall components.

1.4 Aim of this thesis

Although many experimental results in earlier studies have suggested the localization of xylan in the cell wall of hardwood, the deposition mode and the mechanism of cell wall assembly are still unclear. In this thesis, therefore, the following cytochemical studies were performed.

Immunolocalization of xylan in differentiating xylem was examined in Chapter 2. The anti-xylan antiserum was prepared and characterized. The differentiating xylem of *Fagus crenata* was labeled with anti-xylan antiserum and observed by light microscopy and transmission electron microscopy.

Fibrils observed by electron microscopy are not necessarily composed of just cellulose. Hemicellulose, especially xylan, would associate with cellulose fibrils and causes their structural changes. The differentiating fiber of *Fagus crenata*, therefore, was labeled with anti-xylan antiserum and observed using field emission scanning electron microscopy in Chapter 3.

The xylan localization was also examined by selective extraction with the mild delignification and xylanase degradation. The degree of delignification and specificity of xylanase degradation were examined and extensive swelling of secondary wall after xylanase degradation was discussed in Chapter 4. Ultrastructural changes in cell wall after delignification and xylanase degradation were discussed in Chapter 5.

Chapter 2

Immunolocalization of xylan in xylem tissue of *Fagus crenata*

2.1 Introduction

Distribution of hemicellulose has been studied by various methods. Meier and Wilkie (1959) and Meier (1961) estimated very roughly the proportions of individual polysaccharides in each cell wall. They divided a differentiating tissue into four different fractions of cells with the aid of a polarized microscope and a micromanipulator, and determined the sugar composition of these four fractions. Then, they calculated the sugar composition of each cell wall layer as a difference between two fractions. They observed that the xylan content in birch fibers increased at first, reaching a maximum in the S_2 -forming fibers, and then decreased again in the fully developed fibers. The distribution of cell wall polysaccharides, however, could not be precisely determined by Meier's method because the calculation based on the hypothesis that the density of each cell wall layer is the same and the proportion of cell wall polysaccharides in each cell wall layer never changes.

In situ labeling techniques were therefore used to determine the distribution of xylan within the cell wall. Vian et al. (1983) developed xylanase-gold complex as a affinity probe for xylan. They revealed the preferential localization of xylan in the S_1- S_2 transition layer of linden wood fibers (Vian et al. 1986). They assumed that xylan acts as a twisting reagent for cellulose microfibrils forming helicoidal alignment in the S_1- S_2 transition layer. Northcote et al. (1989) prepared anti-β-xylo-oligosaccharide antiserum and revealed that xylan localized only in the secondary wall thickening of mesopyll cells of cultures of *Zinnia elegans* by immunogold labeling.

Cytochemical study with xylanase-gold labeling or anti-xylan immunogold labeling revealed that xylan located only in the secondary wall in dicotyledon. Most of these works, however, did not show the deposition of xylan during the cell wall formation in detail. In this Chapter, therefore, xylan deposition was revealed by immunogold labeling and observed from cambial cells to differentiated cells under light and electron

microscopes. The mode of xylan deposition during cell wall formation was discussed (Awano et al. 1998).

2.2 Materials and Methods

2.2.1 Preparation of oligosaccharides / carrier conjugates

Xylan (glucuronoxylan) from *Fagus crenata* Blume was generously donated by Dr. T. Watanabe (Wood Research Institute, Kyoto University, Japan). Oligosaccharides were prepared from xylan by partial acid hydrolysis in 0.1 M H_2SO_4 at 100 °C for 2 h. The reaction mixture was neutralized with 0.1 M $Ba(OH)_2$ and centrifuged to remove the precipitate. Supernatant was lyophilized and dissolved in distilled water. The oligosaccharide solution was applied to a Bio-Gel P2 column and eluted with water. An aliquot of each fraction was spotted onto a TLC plate and developed by the following solvent; isopropanol : ethanol : H_2O = 7 : 1 : 2. Fractions containing oligosaccharides with a degree of polymerization between 3-6 were combined and lyophilized again.

Oligosaccharides were coupled to keyhole limpet hemocyanin (KLH) by reductive amination method according to Roy et al. (1984). Oligosaccharides (20 mg) and KLH (20 mg) were dissolved in 1ml of 0.2 M borate buffer (pH. 9.0) containing 20 mg of cyanoborohydoride. The reaction was carried out with continuous stirring at 50 °C for 5 days. The reaction mixture was neutralized to pH 4.0 with 80% acetic acid, and dialyzed against distilled water for two days. The solution containing the oligosaccharides / KLH conjugate was then lyophilized and dissolved in 1ml of distilled water. The solution of the conjugates was purified on a Bio-Gel P2 column to separate unreacted oligosaccharides. The fractions containing the conjugates were collected and lyophilized, and the conjugates were dissolved in PBS (1mg/ml) and stored at -80 °C.

2.2.2 Immunization

Eight week old BALB/c female mice were immunized. Before the first immunization, pre-immune sera were taken from each mouse. The initial injection was carried out intraperitoneally with the mixture of 100 μl of the conjugates and 100 μl of Freund's complete adjuvant (FCA). This intraperitoneal injection was repeated twice at 2-week intervals in the same way using Freund's incomplete adjuvant (FIA). Another injection with a mixture of 100 μl of xylan solution (1mg/ml) and 100 μl of FIA followed 2 weeks later, and was repeated twice at 2-week intervals. Three days after the final injection, 300 μl of antiserum was taken from one of the immunized mice and used for the following immunoassays.

2.2.3 Dot-blot Immunoassay

The antibodies were detected by dot-blot immunoassay using positive charged nylon membrane, Biodyne B (Pall corporation; East Hill, NY), as immunoadsorbent. All the procedures described below were performed at room temperature. A sheet of Biodyne B membrane was placed in a dot-blot manifold (Samplatec; Osaka, Japan). Antigen solution containing glucuronoxylan was made up in 2M $NaHCO_3$ at 1mg/ml concentration. The membrane in the manifold was washed in 2M $NaHCO_3$ and 100 μl of various diluted antigen solutions (1-64 fold) was applied to the wells (1.6-100 μg/ dot). Solutions were aspirated with a handy vacuum pump, then all the wells were washed with 100 μl of PBS-T (PBS containing 0.1% (V/V) Tween 20) in the same manner. To avoid nonspecific antibody-binding, all wells were blocked with 3 % (w/v) skim milk in PBS-T (100μl). After the wells were washed four times with PBS-T, 100 μl of various diluted antisera (100-25600 fold) were applied to the wells without aspirating. At the end of 1h incubation, the wells were washed thoroughly with PBS-T and then the membrane was removed from the manifold. The membrane was again washed with PBS-T and then incubated for 1h with goat anti-mouse IgG(H+L)-alkali

phosphatase conjugate (diluted 1:4000 in 3% skim milk in PBS-T). After the membrane was again washed with PBS-T, the bound antibodies were visualized using NBT/BCIP as substrate. Color development was stopped by incubation with 50mM EDTA and the membrane was washed with deionized water.

2.2.4 Light microscopy (Immunogold-silver enhancement)

A *Fagus crenata* tree grown in the Kyoto University Forest in Ashiu (Miyamacho, Kyoto, Japan) was used in this study. Small pieces containing differentiating xylem were cut from the stem and fixed in 3% glutaraldehyde in 1/15M phosphate buffer at pH 7.2 overnight at 4 ℃. The pieces were washed six times with the buffer, dehydrated through a graded ethanol series and embedded in epoxy resin. Transverse sections (1μm thick) were cut from the embedded block and mounted on glass slides. The following immunolabeling procedures were performed on these slides. All the procedures described below were performed at room temperature unless otherwise noted. Sections were incubated for 15 min with 50 mM glycine in PBS. After three washes in PBS, they were incubated for 30 min with 3% skim milk in PBS-T to avoid nonspecific antibody binding. At the end of the incubation, sections were washed three times for 5 min each time in PBS-T, then incubated in the antiserum (diluted 1:100 in 3% skim milk in PBS-T) for 2 hours at 37 ℃. For the control experiment, the serial sections were incubated in either normal serum (1:100 dilution) taken before the first immunization or in the antiserum previously incubated with xylan (1mg/ml). After the incubation, sections were washed three times for 5 min each in PBS-T and then incubated in Auro Probe GAM G15 (Amersham; UK) diluted 1:25 in PBS for 2h at 37 ℃. They were again washed three times for 5 min each in PBS-T and fixed with 2% glutaraldehyde in PBS for 5 min, after which they were washed with distilled water. To detect the labeling under a light microscope, the sections were treated in an Inten SE M Silver enhancement kit (Amersham) for 15-20 min. Reaction was stopped by washing with distilled water and

observation was made under a light microscope without any dye-staining.

2.2.5 Electron microscopy (Immunogold labeling)

Ultrathin sections were prepared sequentially from the embedded specimen which was used for the preparation of light microscopic sections, and mounted on 75 mesh Ni grids. The procedures described below were performed at room temperature unless otherwise noted. The sections on grids were immersed in 50 mM glycine in PBS for 15 min. After three washes in PBS, they were incubated in blocking buffer (PBS containing 0.8% BSA, 0.1% IGSS quality gelatin (Amersham), 5% goat serum and 2 mM NaN_3) for 30 min, then washed three times for 5 min each in washing buffer (same as blocking buffer but without goat serum) and incubated in antiserum for 2h at 37 °C. For the control experiment, serial sections were incubated in pre-immune serum or antisera previously incubated with one of the following saccharides: xylose, xylobiose, xylotriose, glucuronoxylan, pectin, xyloglucan, or glucomannan. Sections were then washed in washing buffer three times for 5 min each and incubated in Auro Probe GAM G15 diluted 1:25 in blocking solution for 2h at 37 °C. They were washed in washing buffer three additional times and fixed with 2% glutaraldehyde in PBS for 5 min, after which they were washed with distilled water, stained with 2% aqueous uranyl acetate and Reynolds' lead citrate and examined with a TEM (JEM-2000 ES, JEOL) at 100kV.

2.3 Results

2.3.1 Specificity of anti-xylan antiserum

The result of dot-blot immunoassay is shown in Fig. 2.1. Color developments were proportional to the concentration of antigen or antiserum. This development was not observed when the dots were incubated with PBS, nor was any color development seen

in the dots which had not absorbed xylan.

When the ultrathin sections were treated with the antiserum, many gold particles were seen in the secondary wall but not in the primary wall or the middle lamella (Fig. 2.2A). However, gold particles were seldom found in the sections treated with the antiserum pre-incubated with xylan (Fig. 2.2B). When xylotriose or xylobiose was used as a competitor, the immunogold labeling was almost completely inhibited (Fig. 2.2C). Fewer gold particles were observed when the antiserum was pre-incubated with xylose (Fig. 2.2D). Pectin, xyloglucan and glucomannan did not inhibit labeling (Fig. 2.2E), and labeling was rarely found when the sections were treated with pre-immune serum (Fig. 2.2F). Results of the competitive inhibition test are summarized in Table 2.1.

2.3.2 Xylan localization at tissue level (Light microscopy)

Labeling was seen in the secondary wall of differentiating xylem (Fig. 2.3) and their intensity increased in the course of cell wall formation. The cell walls in the cambial zone and expansion zone were not labeled. At high magnification, no labeling was found in the lumen, compound middle lamella or pit chambers (Fig. 2.4).

2.3.3 Xylan localization at cellular level (Electron microscopy)

Gold particles were found only in the secondary walls of xylem elements, i.e., vessel elements, fibers, axial parenchyma and ray parenchyma. In mature fibers, vessel elements and axial parenchyma, these particles were evenly distributed throughout the secondary wall, except for the outer part of the S_1 layer in which they were less abundant (Figs. 2.5, 2.6). No labeling was found in the cell walls during expansion growth (Fig. 2.7A). In the S_1 forming fibers, labeling was found in the inner part of the S_1 layer but not in the outer part (Fig. 2.7B), while in the S_2 forming fibers, labeling was found in the inner part of the S_1 layer and in the S_2 layer (Fig. 2.7C) . Labeling density of the S_2 layer was the same extent to that of the inner part of the S_1 layer (Fig. 2.7C). Gold particles in the

S_1 and S_2 layers were more abundant during the S_3 formation stage of fiber than those during the S_2 formation stage (Fig. 2.7D). In the fibers which had completed the S_3 layer formation, labeling still increased in all cell wall layers (Fig. 2.7E).

2.3.4 Quantification of labeling

The variation in labeling density during cell wall formation is shown in Fig. 2.8. The number of labelings per square μm in the S_1, S_2 and S_3 layers increased during cell wall formation.

2.4 Discussion

Histochemical localization of xylan was revealed by the immunogold silver enhancement technique. Labeling was observed only in the secondary wall of xylem cells, i.e. vessel elements, wood fibers, axial parenchyma and ray parenchyma (Fig. 2.3). The cell walls in the cambial zone and cell expansion zone were not labeled (Fig. 2.3). At high magnification, no labeling was found in the lumen, compound middle lamella or pit chambers (Fig. 2.4). These results suggest that xylan distribution was limited to the secondary wall. The intensity of labeling increased in the course of cell wall formation. This result implies that xylan content in the secondary wall gradually increase during the secondary wall maturation.

Electron microscopic observation also showed labeling was only in the secondary wall of xylem elements. In mature fibers, vessel elements and axial parenchyma, gold particles were found throughout the secondary wall, though few particles were observed in the outer part of the S_1 layer (Fig. 2.5, 2.6). There are two possible explanations for the less abundant labeling in this region: the antigenic sites in this region may be masked by phenolic components such as lignins, or xylan may actually be less abundant. The former possibility is probably less likely, because few particles were found in the S_1

layer of differentiating fibers which were not lignified. Therefore, masking of antigenic sites would not occur in this specimen. The results in this Chapter differ from those of the studies using the enzyme-gold method by Vian et al. (1983, 1986, 1992). They found that the labeling of xylan was preferentially localized in the transition zone S_1-S_2. This difference may be due to the difference of specificity between antibodies and xylanase. On the basis of chemical extraction, Vian et al. (1986) suggested that there are two kinds of xylan: one encrusting the overall secondary wall is strongly bound to cellulose microfibrils and the other is embedded in the cellulose microfibrils of the transition zone. The antiserum used in this study could bind to both types of xylan, while the xylanase-gold complex was able to recognize only the latter one.

Labeling density increased during the cell wall formation. For example, in the fibers which had just completed the S_3 layer formation, the labeling densities in the S_1 and S_2 layers were 12.2 and 15.5 particles/μm^2, respectively (Fig. 2.8). The densities increased to 20.7 and 26.7 particles/μm^2, respectively, in the fibers which located farther from the cambium (Fig. 2.8). These results imply that the deposition of xylan into the cell wall occurs continuously after the S_3 formation. Xylan is synthesized in the Golgi apparatus and transported to the cell wall as well as other hemicelluloses (Northcote et al. 1989; Suzuki et al. 1991; Baydoun and Brett 1997). Therefore, the increase of xylan in the cell wall layer implies that xylan would be able to penetrate through the cell wall layers, i.e. xylan deposits to the cell wall by intussusception.

From radio tracer experiments using ^{14}C-glucose, Takabe et al. (1981) suggested that xylan deposition was active between the later part of S_1 stage and the beginning part of S_2 stage, and between the final part of S_2 stage and S_3 stage. They hypothesized that xylan deposits in the outer part of S_2 layer and S_3 layer. The hypothesis, however, excluded the deposition by intussusception. The xylan synthesis during the final part of S_2 stage and S_3 stage would cause the increase of the labeling density in the S_1 and S_2 layers.

2.5 Abstract

Antiserum against xylan has been raised to mice. The dot-blot immunoassay revealed that the antiserum recognizes xylan. Competitive inhibition test using xylem tissue indicated that the antiserum could bind specifically to β-1,4-D-xylose moiety of xylan but not to other polysaccharides such as glucomannan, xyloglucan and pectin. The antiserum, therefore, was used for immunogold-labeling to investigate the localization of xylan in differentiating xylem of *Fagus crenata* Blume.

For light microscopy, sections were labeled by immunogold silver enhancement methods using anti-xylan antiserum as a primary antibody. Labeling was observed in the secondary wall of xylem cells, that is, vessel elements, wood fibers, axial parenchyma and ray parenchyma, but was not found in the compound middle lamella, pit chambers or cell lumen of these cells. The cell walls in the cambial zone and cell expansion zone were not labeled.

To examine the distribution of xylan at a subcellular level, ultrathin-sections were observed under a transmission electron microscope. The labeling of xylan was observed only in the secondary walls of xylem cells, but not in the primary walls and the middle lamella. Xylan was evenly distributed in the secondary walls except for the outer part of the S_1 layer in which it was less abundant. The labeling density in each secondary wall layer (S_1, S_2 and S_3) increased during the cell wall formation. This result suggests that the deposition of xylan occurs in a penetrative way.

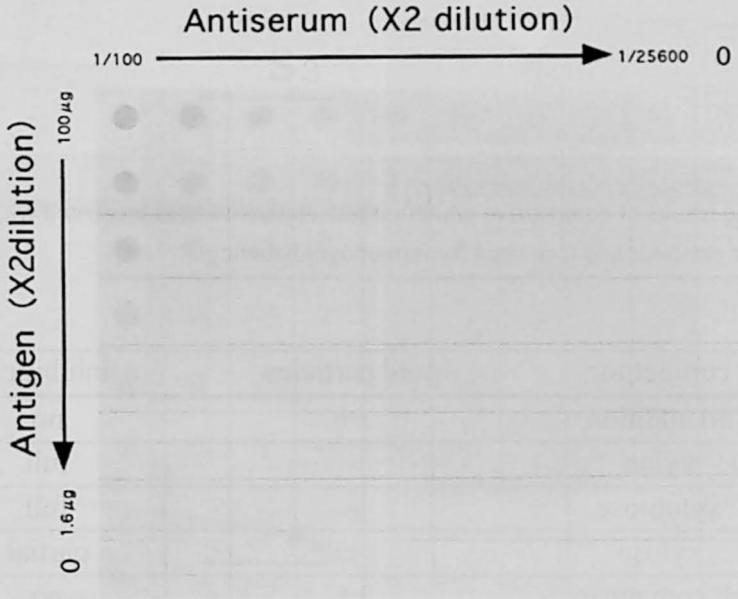

Fig. 2.1

The specificity of antiserum was examined by dot-blot immunoassay. Color development gradually decreased according to the dilution of antiserum and/or antigen. No color development was observed in the dots which did not absorb xylan (bottom lane). When the antiserum incubation was omitted, color development was not observed (extreme right lane).

Table 2.1

Summary of the results of competitive inhibition test. Antiserum was incubated with one of the various competitors for one hour and then used for immunogoldlabeling.

competitor	gold particles	inhibition
no addition	++	no
xylan	-	full
xylobiose	-	full
xylose	+	partial
glucomannan	++	no
xyloglucan	++	no
pectin	++	no

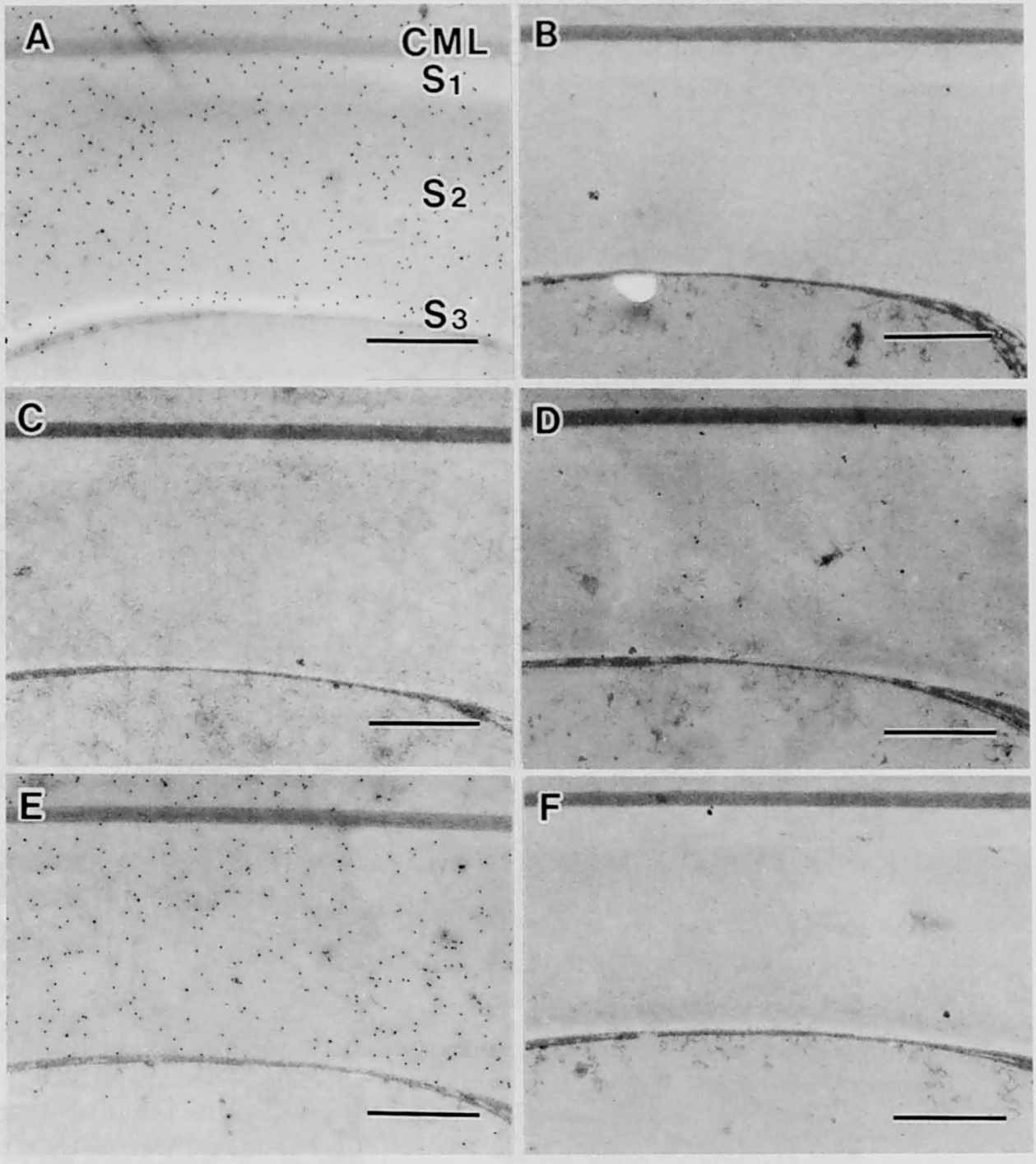

Fig. 2.2

Six serial ultrathin sections were immunolabeled with various sera; **A** Anti-xylan antiserum, **B** Anti-xylan antiserum previously incubated with xylan, **C** Anti-xylan antiserum previously incubated with xylobiose, **D** Anti-xylan antiserum previously incubated with xylose, **E** Anti-xylan antiserum previously incubated with xyloglucan and **F** pre-immune serum. Xylan, xylobiose and xylose inhibited the antiserum from binding the sections though xyloglucan did not. CML, *compound middle lamella*; S_1, *outer layer of secondary wall*; S_2, *middle layer of secondary wall*; S_3, *inner layer of secondary wall.* Bars = 1μm.

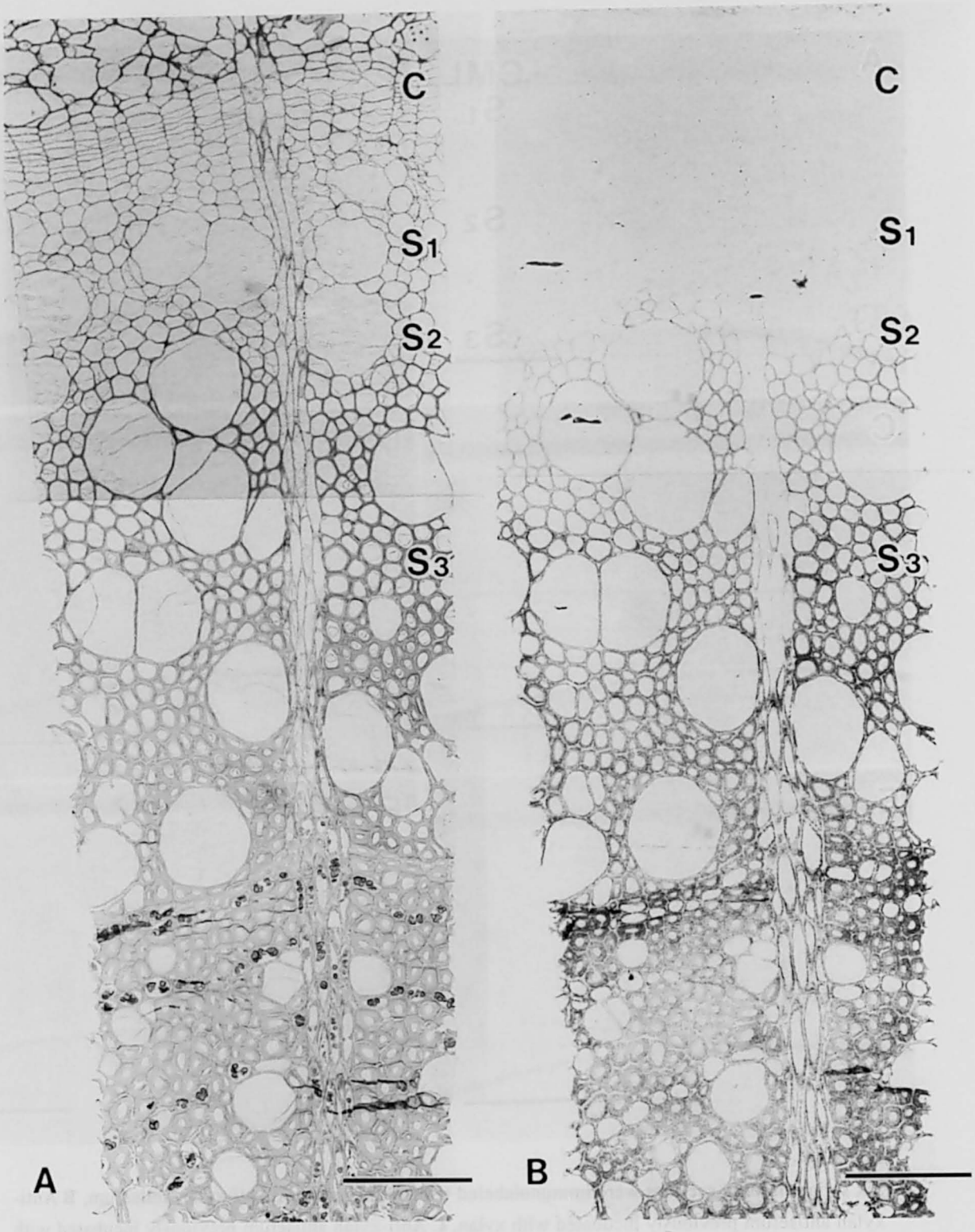

Fig. 2.3

Serial sections were cut, and some of them were stained with 1% safranin (**A**) and others labeled with antiserum (**B**). In the sections labelled with antiserum, labelling was seen in the cell wall of xylem elements, i.e.,vessel elements, fibers, axial parenchyma and ray parenchyma. C, *cambial zone* ; S_1, S_2 and S_3, *the starting position of corresponding cell wall layer formation.* Bars = 100μm.

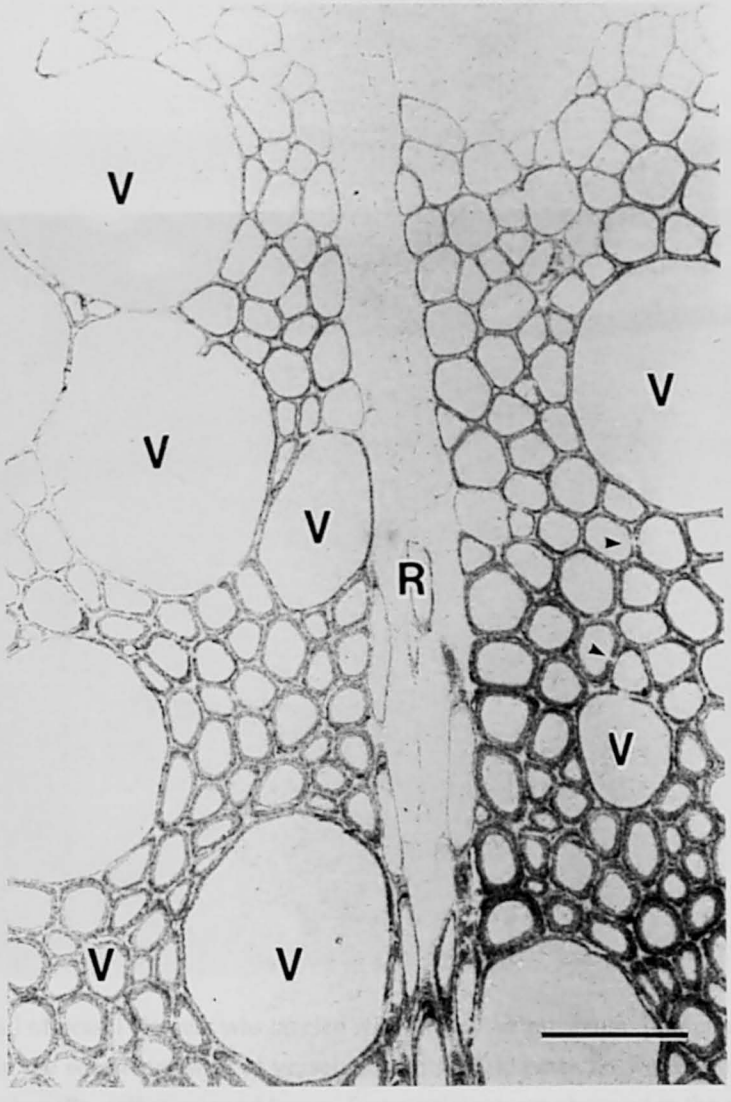

Fig. 2.4

Labeled sections were observed under a light microscope at high magnification. No labelling was found in the lumen, compound middle lamella and pit chambers (arrowheads). Density of labelling increased in the course of cell wall formation. V, *vessel element*; R, *ray parenchyma.* Bar = 50μm.

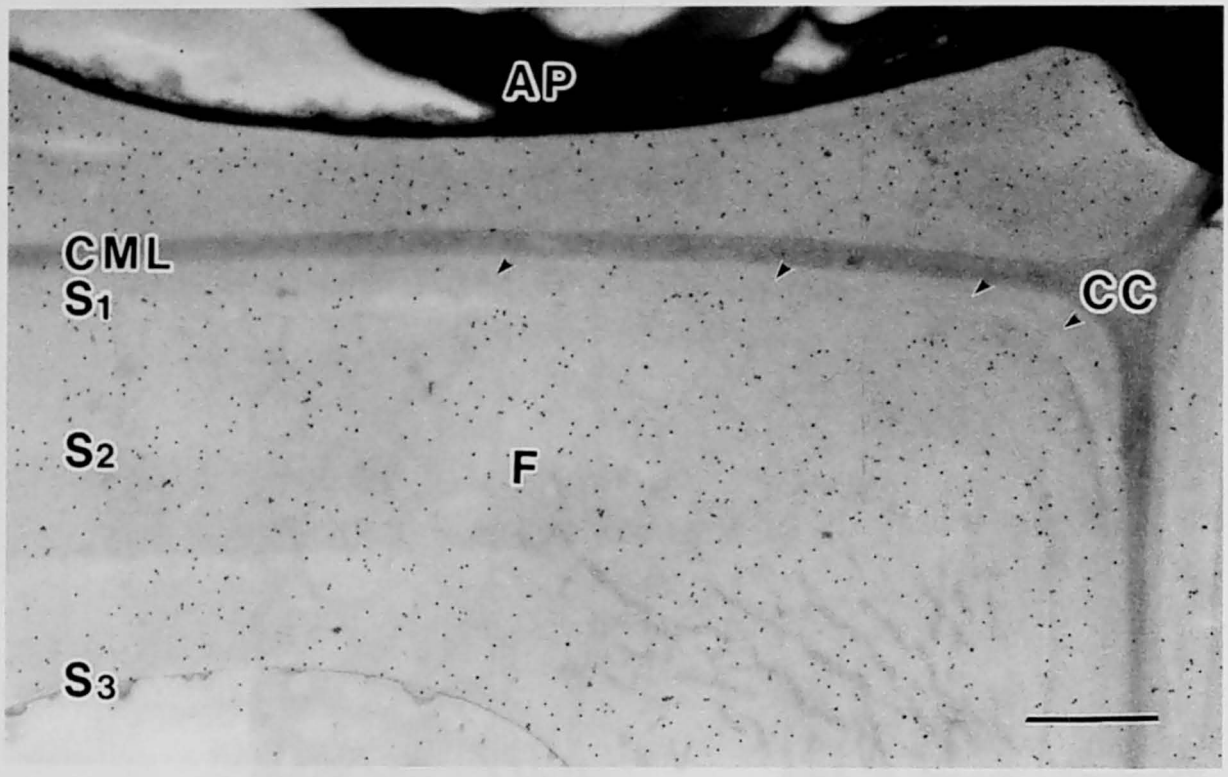

Fig. 2.5

Immunogold labeling was found only in the secondary wall of fiber (F) and axial parenchyma cell (AP). Gold particles were rarely found in the compound middle lamella, cell corner and lumen. Particles were evenly seen in the secondary wall except that few particles were seen in the outer part of the S_1 layer (arrowheads). CML, *compound middle lamella*; S_1, *outer layer of secondary wall*; S_2, *middle layer of secondary wall*; S_3, *inner layer of secondary wall*; CC, *cell corner middle lamella.* Bar = 1μm.

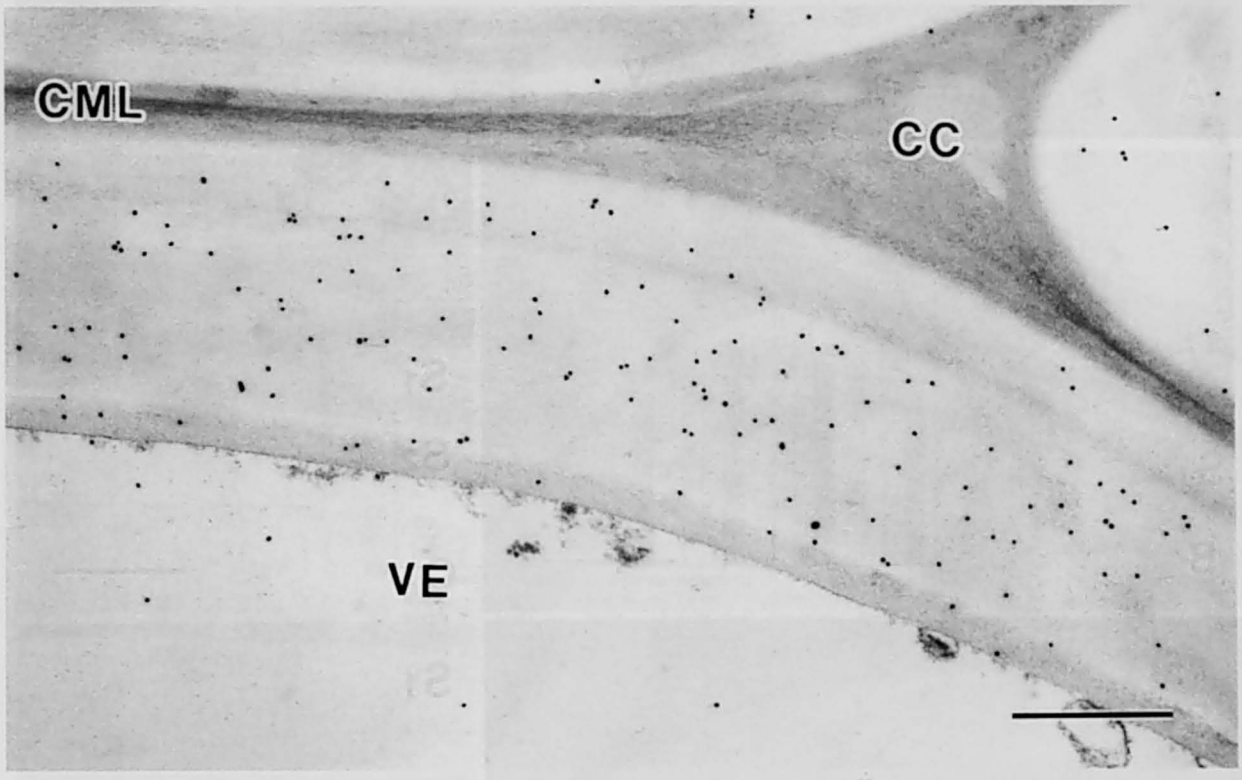

Fig. 2.6

The secondary wall of vessel element was labeled with anti-xylan antiserum. Immunogold labeling was also found only in the secondary wall of vessel elements. Gold particles were scarcely found in the compound middle lamella, cell corner and lumen. Few particles were observed in the outer part of the S_1 layer. VE, *vessel element*; CML, *compound middle lamella*; CC, *cell corner middle lamella.* Bar = 0.5μm.

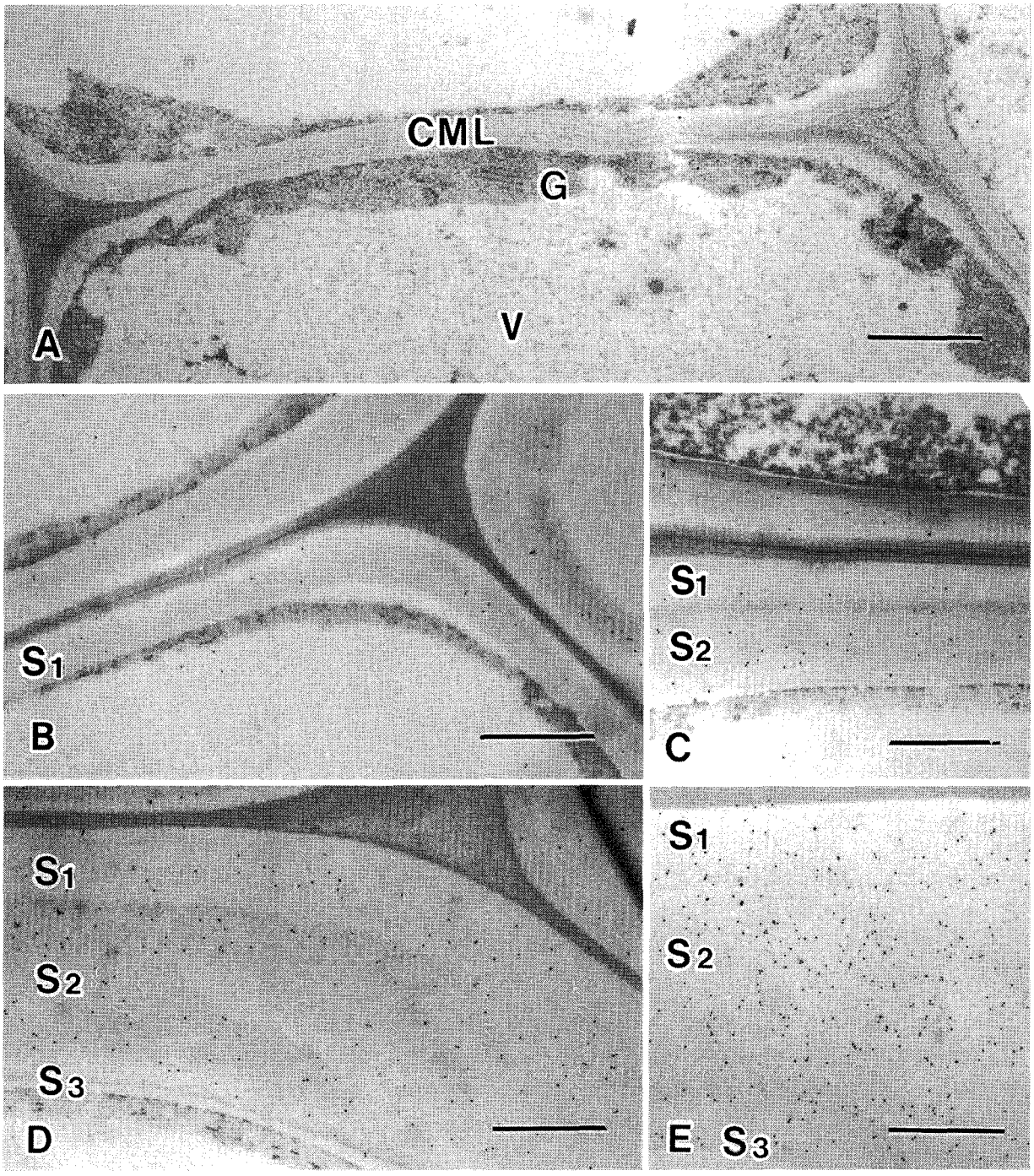

Fig. 2.7

The differentiating fibers at various stages were labeled with anti-xylan antiserum. **A** Cells in cambium zone. Labelings were hardly found in the cell wall and cytoplasm. **B** The S_1-forming fiber. Labels were found in the secondary wall of the S_1-forming fiber. The number of labels in the S_1 layer was less than that of matured fibers (compare with Fig. 2.5). **C** The S_2-forming fiber. Gold particles were found in the inner part of the S_1 layer and in the S_2 layer, though few were found in the outer part of the S_1 layer. Label was not seen in the primary wall, middle lamella and cytoplasm. Note that the number of particles in both the S_1 and S_2 layers was less than that of matured fibers (compare with Fig. 2.5). **D** The S_3-forming fiber. Labels were found in overall secondary wall except for the outer part of the S_1 layer. Label was rarely seen in the primary wall, compound middle lamella and cytoplasm. Note that the number of particles in both the S_1 and S_2 layers was less than that of the matured fibers (compare with Fig. 2.5). **E** The S_3 -formed fiber. Label was found in overall secondary wall except for the outer part of the S_1 layer. Label was rarely seen in the primary wall and compound middle lamella. Note that the number of particles in both the S_1 and S_2 layers was more than that of the S_3-forming fibers. V , *vacuole*; G , *Golgi apparatus*; CML, *compound middle lamella*; S_1, *outer layer of secondary wall*; S_2, *middle layer of secondary wall*; S_3, *inner layer of secondary wall.* Bars = 0.5μm.

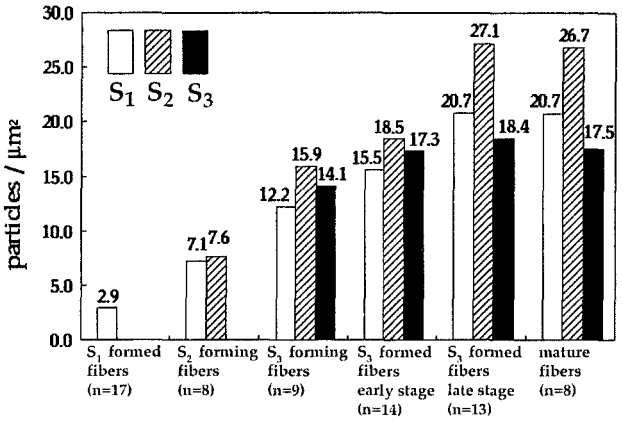

Fig. 2.8

The number of gold particles per unit of cell wall area was calculated from electron micrographs taken from one of the labeled sections. The labeling density in the S_1 layer is always lower than that of the S_2 layer beause there are few labeles in the outer part of S_1 layer. The labeling density in the S_1, S_2 and S_3 layers gradually increased during the cell wall formation. Interestingly, that in the S_1 and S_2 layer increased continuously after the deposition of cellulose microfibrils in the S_3 layer. Numbers in parentheses indicate the number of cells calculated.

Chapter 3

Deposition of xylan on *Fagus crenata* fiber observed by immuno scanning electron microscopy

3.1 Introduction

Most of the information on the three dimensional ultrastructure of cell walls of higher plants has been provided by replica techniques involving rapid freezing and deep etching (RFDE) methods (McCann and Roberts 1991, 1994, Satiat-Jeunemaitre et al. 1992, Itoh and Ogawa 1993, Nakashima et al. 1997, Fujino and Itoh 1998, Hafrén et al. 1999). Although the replica technique is very useful for observations on plant surface structure at high resolution, it is not possible to identify what types of molecules constitute the observed structures because a suitable staining technique has not so far been developed.

Suzuki et al. (1998) reported the localization of xyloglucans in the cell walls of tobacco culture suspensions using RFDE coupled with immunogold labeling. The application of immunogold method for replica technique overcomes the defect mentioned above. Although the auther applied this technique to the immunolocalization of xylan in secondary cell walls, good results were not obtained because of the difficulty of retaining gold particles on the replica membranes during the dissolution of organic materials. In addition, specimens required heavier coating with platinum and carbon for retention of gold labels on the replica, which may cause poor images of the specimen.

The progress and development in field emission scanning electron microscopy (FESEM) allows for high resolution images of cell walls equivalent to those observed with replica techniques (Abe et al. 1991, 1992). Since the resolution of FESEM is adequate to detect colloidal gold as small as 5 - 20 nm (Pawley 1997, Takata et al. 1988, Osumi et al. 1992, Suzuki et al. 1994, Osawa et al. 1999), the immuno FESEM technique represents a potentially powerful method for *in situ* identification of molecules on specimen surface.

In this Chapter, immunogold labeled sections from *Fagus crenata* Blume were observed by a FESEM. Changes in ultrastructure of the secondary wall during cell wall formation and the deposition of xylan are discussed (Awano et al. 2000).

3.2 Materials and Methods

3.2.1 Plant material

During the active growth period, small blocks containing differentiating xylem were taken from a living tree of *Fagus crenata* Blume grown in the Kyoto University Forest in Ashu (Miyamacho, Kyoto, Japan). Blocks were fixed and stored in 3% glutaraldehyde in 1/15 M phosphate buffer at pH 7.2.

3.2.2 Immunogold labeling

Specimen blocks were washed with distilled water and sectioned on a sliding microtome. Radial sections (100 μm thick) were incubated for 15 min at room temperature on 50 mM glycine in phosphate buffered saline (PBS). After three washes in PBS, they were incubated for 30 min at 37 °C in blocking buffer (PBS containing 0.8% bovine serum albumin, 0.1% immunogold silver-staining (IGSS) quality gelatin (Amersham), 5% goat serum and 2 mM NaN_3). After the incubation, sections were washed 3 times for 10 min each in washing buffer (same as blocking buffer but without goat serum). The preparation and specificity of the mouse antiserum against xylan used in this study was previously described in Chapter 2. Sections were incubated for 2 h at 37 °C in anti-xylan antiserum at 1:100 dilution in blocking buffer. As a control, pre-immune serum taken before immunization was used for labeling instead of the anti-xylan antiserum. After six gentle washes of 10 min each in washing buffer, sections were incubated for 2 h at 37 °C in 5 nm colloidal gold conjugated goat anti mouse IgG secondary antibody (Auro Probe GAM G5, Amersham) diluted at 1:25 in blocking buffer. At the end of incubation, non reacting antibodies were thoroughly removed by three washes of 10 min each in blocking buffer and six washes of 10 min each in PBS. Sections were refixed for 5 min in 3% glutaraldehyde in PBS and washed three times in 1/15 M phosphate buffer at pH 7.2.

3.2.3 FESEM observation

Sections labeled with antiserum were treated with 2% osmium tetroxide in 1/15 M phosphate buffer for 2 h at room temperature. Thereafter sections were dehydrated through a graded ethanol and acetone series and dried using a critical point dryer (E-3000; Polaron) with liquid CO_2 as the drying agent. Dried sections were coated with platinum-palladium (about 1 nm thick) using a high resolution sputter coater (Agar, UK). Sections were examined using a FESEM (S-4500; Hitachi, Japan) at an accelerating voltage of 15 kV.

3.2.4 Determination of fibril width

FESEM images were recorded on a black and white negative film (T-max 400; Kodak) and enlarged on photographic paper at 200,000 x. One hundred fibrils were selected at random from a 1.0 μm x 1.0 μm field and their corresponding width was measured.

3.3 Results

3.3.1 Deposition of microfibrils in the secondary wall of differentiating fibers

Fibers in different growth stages were observed, i.e. those in the S_1- and S_2-forming stages as well as mature fibers. Very few fibers in S_3-forming stages were visible in the sections.

When a fiber was observed from the lumen, cytoplasm was often found on the surface of the cell wall (Fig. 3.1). The newly deposited cell wall which was located beneath the cytoplasm was, however, easily distinguishable from the sliced cell wall. Figure 3.1 shows the inner surface of a fiber cell wall in the S_1 forming stage. Sparsely deposited fibrils are apparent and oriented in a Z-helix at about 45° to the fiber axis. The width of the fibrils varied between 4.8 and 14.3 nm while most of thick fibrils were approximately

12 nm wide (Fig.3.7). Thick fibrils were composed of fine fibrils (5 nm), and some thick fibrils aggregated to form bundles (Fig. 3.2 arrows). The fibrils appeared wavy rather than straight.

Occasionally, the S_1 layer of fibers in the S_2-forming stage was exposed by removal of the S_2 layer (Fig. 3.3). Here the fibrils were deposited densely and highly oriented at about 45° to the fiber axis. Interfibrillar spaces were very narrow and straight (Fig. 3.3). Most of the fibrils were 12.7 nm wide, and the variation in the fibril width was quite small.

On the inner surface of the cell wall in S_2-forming fibers, fibrils were deposited densely and oriented almost parallel to the fiber axis (Figs. 3.4, 3.5). Their width varied between 11.4 and 20.3 nm with the average being 15.7 nm (Fig.3.7) .

The internal part of the S_2 layer was exposed where the cell wall was sliced. Fibrils are deposited densely and highly oriented almost parallel to the fiber axis (Fig. 3.6). Their average width was 15.7 nm. Interfibrillar spaces were very narrow and fibrils were located very close to each other (Fig. 3.6).

The variation in fibril width found in the S_1 and S_2 cell wall layers is shown in Fig. 3.7.

3.3.2 Anti-xylan immunogold labelling

Fagus crenata sections treated with anti-xylan antiserum showed strong labeling, and many particles, approximately 17 nm in size, attached to both the inner surface (Fig. 3.8A) and the sliced surface of the secondary wall (Fig. 3.8B). Very few particles were observed on sections treated with pre-immune serum as an immunocytochemical control (Figs. 3.8C, D).

On the inner surface of the cell wall in S_1 forming fibers, labels were found on thick fibrils but not on the fine fibrils (Fig. 3.2). These labels tended to be attached to the bundles of thick fibrils (Fig. 3.2). Immunolabeling of the S_1 layer of S_2 forming fibers

was more abundant than that observed on the newly formed S_1 layer (Fig. 3.3).

Numerous labels were observed on the inner surface of the secondary wall in S_2-forming fibers (Fig. 3.5). Labels were also found on the sliced surface of the S_2 layer (Fig. 3.6) and their density appeared higher than that in the newly formed S_2 layer (Fig. 3.4).

3.4 Discussion

3.4.1 Ultrastructure of secondary wall during the cell wall formation

On the inner surface of secondary walls in S_1-forming fibers, the fibrils were deposited sparsely and varied in size. Some fine fibrils with a width of 5 nm were aggregated to form thicker fibrils with a width of 12 nm (macrofibrils). The microfibril diameter in various woody plants was estimated as 3.5 nm by TEM observation of permanganate fixed specimens (Kerr and Goring 1975, Ruel et al. 1978, Donaldson and Singh 1998). The fibrils with a width of 5 nm observed in this study would correspond to microfibrils with their slightly thicker size due to the metal coating. Macrofibrils frequently touched neighboring macrofibrils at different points along their axis (Fig. 3.2). Some macrofibrils also aggregated to form bundles. As is often the case with S_1-forming fibers, newly deposited fibrils on the inner surface seem to be unstable and easily peeled from the underlying cell wall (Fig. 3.2). This may represent an artifact formed during fixation or sectioning, although equivalent structures could not be found on the inner surface of S_2-forming fibers. Therefore, the inner surface of S_1-forming fibers might be more unstable and fragile than an equivalent surface in S_2-forming fibers.

In S_2-forming fibers, fibrils deposited more densely on the inner surface of the secondary wall. Microfibrils of 5 nm width were not found and most of the fibrils showing an average width of 15.7 nm were thicker than those present in the S_1 layer.

This may result from the synthesized microfibrils rapidly aggregating to form macrofibrils.

Compared to the inner surface of the secondary wall, the sliced surface of secondary walls showed more packed and straight macrofibrils. The inner surface of the secondary wall represents the swollen polysaccharide gel containing water reported by Terashima et al. (1993). In the course of cell wall maturation, water is gradually removed from the cell wall causing shrinkage of the swollen polysaccharide gel and the formation of tightly packed fibrils. However, the width of fibrils was greater on sliced surfaces than on the inner surface. This result implies that some cell wall components such as xylan and lignin would attach and surround the macrofibrils after their deposition in the wall.

3.4.2 Immunolocalization of xylan

A mixed image of a secondary electron (SE) image and a backscattered electron (BSE) image has frequently used for immuno SEM. A BSE image of a carbon coated specimen gives localizaton of colloidal gold particles because gold particles yields stronger BSE signal than carbon. However, wood sections coated with carbon readily showed charging effects and so well contrasted BSE images could not be obtained. Therefore, specimens in the present study were coated with platinum-palladium alloy and observed as SE image.

By comparing specimens labeled with anti-xylan antiserum (Fig. 3.8A, B) with those of controls (Fig. 3.8C, D), many particles were found on the secondary wall in the former, though no particles were observed in the latter. Most of particles were about 17 nm in size, the other particles were larger than 50 nm (Fig. 3.8C, D). The former represents complex of primary and secondary antibody, the latter may be aggregation of secondary antibody (an artifact). Therefore the about 17 nm wide particles showed localization of the xylan.

On the inner surface of the secondary wall in S_1-forming fibers, immunogold labels

against xylan were localized on the more than 12 nm wide fibrils. According to observations made on isolated xylan by negative staining, xylan is composed of stiff rod-shaped molecules which are ca. 35 nm long and 2 nm wide (Vian et al. 1986). In this study, however, no molecules with this shape were apparent. Therefore, fibrils seen in this study are likely to represent microfibrils or macrofibrils coated with xylan. There was no label found on microfibrils with 5 nm width (Fig. 3.2). These microfibrils represent single cellulose microfibrils, although the possibility that other molecules apart from xylan may be attached cannot be excluded.

Compared to the newly formed S_1 layer (Fig. 3.2), greater labeling was found on the sliced surface of the S_1 layer in S_2 forming fibers (Fig. 3.3). The sliced surface of the S_2 layer also labeled more intensely than the inner surface of the S_2 layer (Fig. 3.4). These results suggest that the deposition of xylan into the cell wall may occur continuously after macrofibril deposition, which supports the results of TEM observation in Chapter 2.

3.5 Abstract

Xylan is localized exclusively in the secondary wall of *Fagus crenata* Blume and gradually increase during the course of fiber differentiation. To reveal where xylan deposits within secondary wall and how xylan affects cell wall ultrastructure, immuno scanning electron microscopy with anti-xylan antiserum was applied in this study.

In S_1-forming fibers, microfibrils were small in diameter and deposited sparsely on the inner surface of the cell wall. Microfibrils with approximately 5 nm width aggregated and formed thick fibrils with 12 nm width (macrofibrils) which labeled positively for xylan. In S_2-forming fibers, macrofibrils were thicker than those found in S_1-forming fibers and were densely deposited. Compared with newly formed secondary walls, previously formed secondary walls were composed of thick and highly packed

macrofibrils. Labels against xylan were much more prevalent on mature secondary walls than on newly deposited secondary walls. This result implies that the deposition of xylan into the cell wall may occur continuously after macrofibril deposition and may be responsible for the increase in diameter of the macrofibrils.

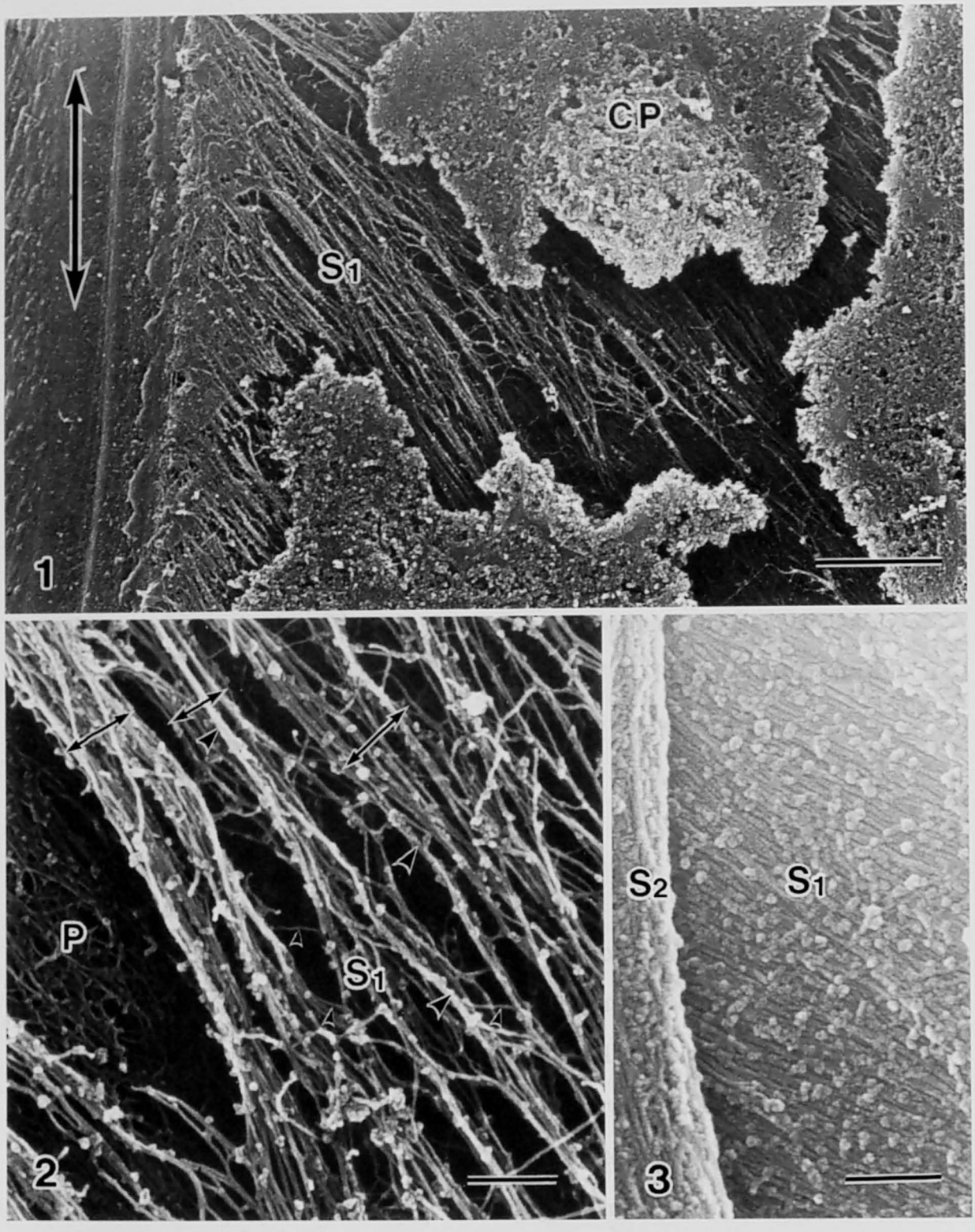

Fig. 3.1 Overview of S_1-forming fiber. Cytoplasm was often found on the inner surface of the secondary cell wall. An arrow indicates direction of fiber axis. Bar = 2 μm.

Fig. 3.2 Inner surface of S_1-forming fiber. Large arrowheads represent macrofibrils and small ones represent microfibrils. Anti-xylan labels were found on macrofibrils but not on microfibrils. Some macrofibrils aggregated together to form bundles (arrows). Bar = 200 nm.

Fig. 3.3 S_1 layer in S_2-forming fiber exposed by sectioning. Macrofibrils were straight and densely deposited. Macrofibrils were thicker than those in Fig. 3.2. Macrofibrils were heavily labeled with anti-xylan antiserum. Bar = 200 nm.
CP, *cytoplasm*; P, *primary wall*; S_1, *outer layer of secondary wall*; S_2 *middle layer of secondary wall*

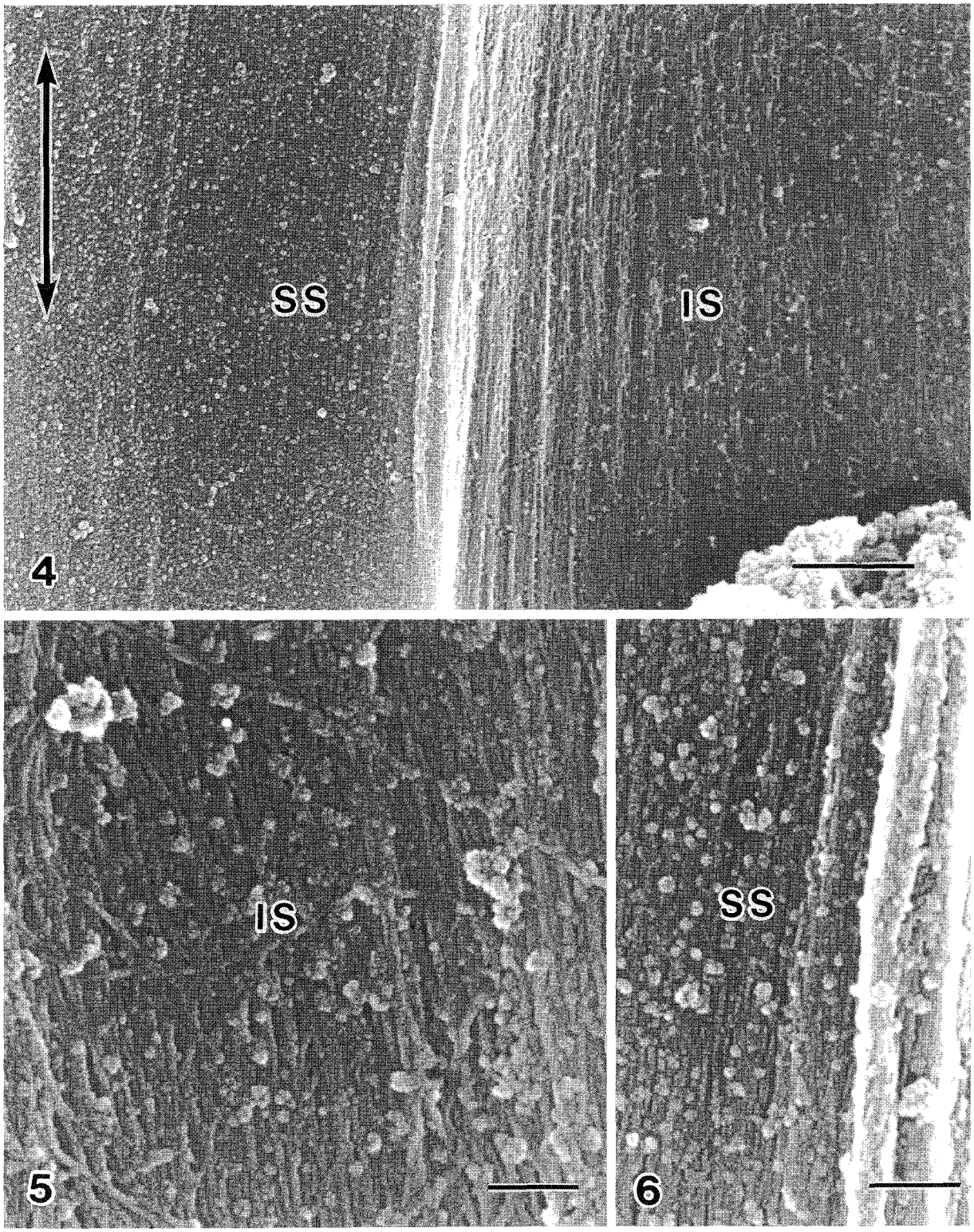

Fig. 3.4 Overview of S_2-forming fiber. Macrofibrils deposited almost parallel to fiber axis. An arrow indicates direction of fiber axis. IS, *inner surface of S_2 layer*; SS, *sliced surface of S_2 layer*. Bar = 1 μm.

Fig. 3.5 Inner surface of S_2-forming fiber. Microfibrils (as seen in Fig. 3.2) were not found. Macrofibrils were thicker than those present in the inner surface of S_1-forming fibers. IS, *inner surface of S_2 layer.* Bar = 200 nm.

Fig. 3.6 Sliced surface of S_2-forming fiber. Note that anti-xylan label was more intense on the sliced surface than on the inner surface (Fig. 3.5). SS, *sliced surface of S_2 layer.* Bar = 200 nm.

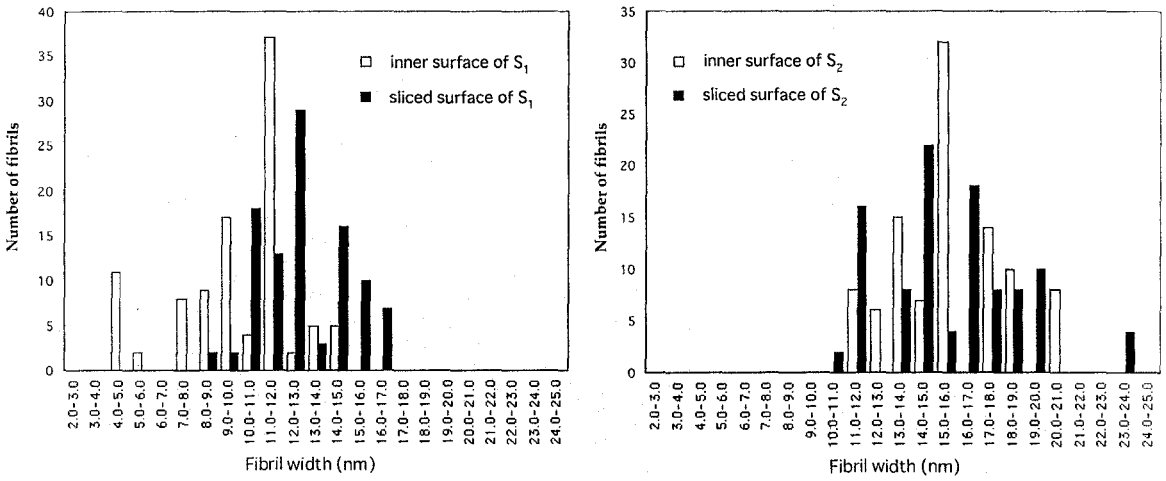

Fig. 3.7

The frequency of fibril width. Fibrils were selected at random from 1.0 μm x 1.0 μm field.

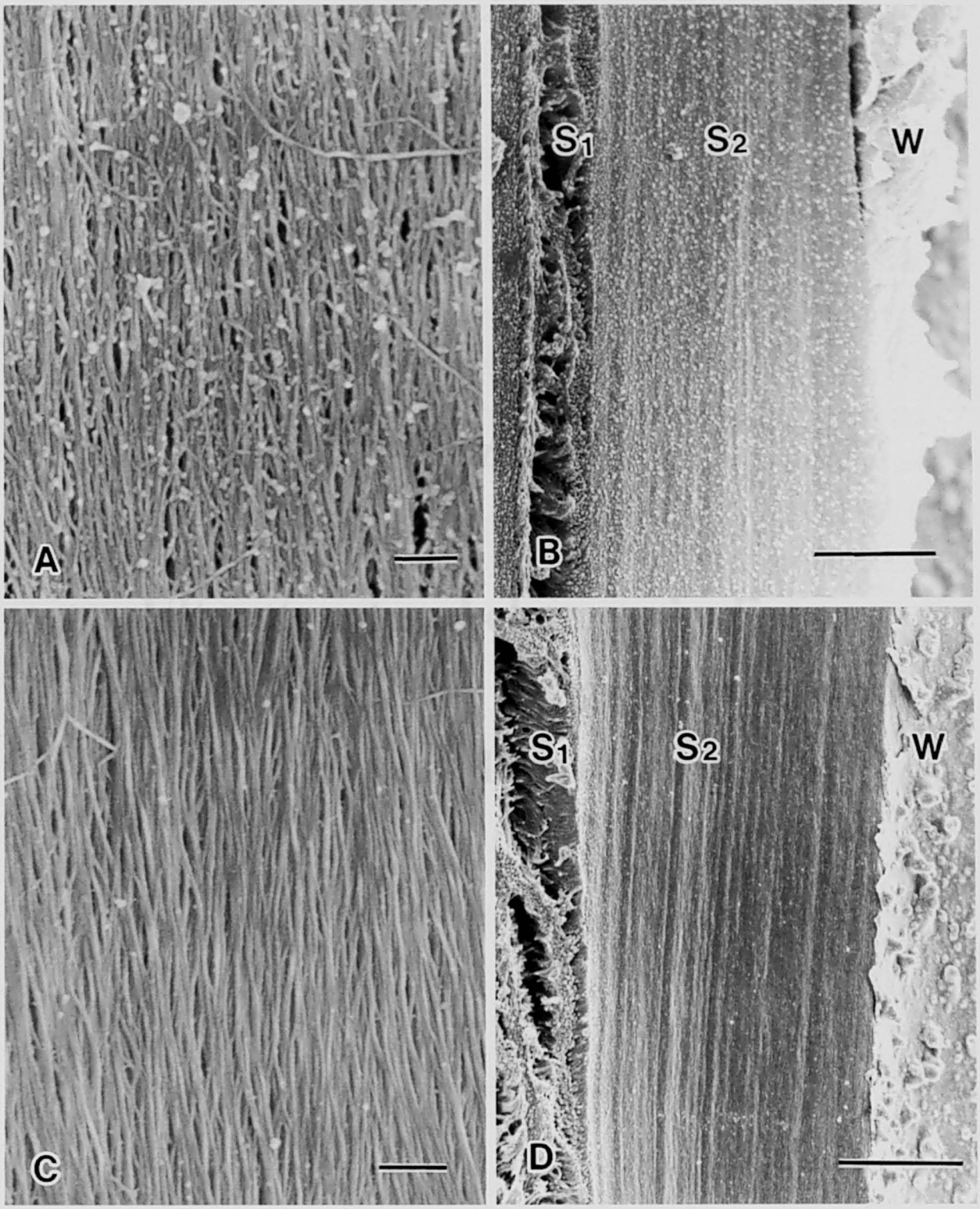

Figs. 3.8

Inner surface of S_2 layer in S_2-forming fiber incubated with anti-xylan antiserum (**A**) and preimmune serum (**C**). Particles with 17 nm width represent anti-xylan labals. Bars: 200 nm. Sliced surface of mature fiber incubated with anti-xylan antiserum (**B**) and preimmune serum (**D**). Particles with 17 nm width showed localization of xylan. S_1, *outer layer of secondary wall (S_1 layer)*; S_2,*middle layer of secondary wall (S_2 layer)*; W, *warty layer*. Bars = 1 μm.

Chapter 4

Ultrastructural changes in *Fagus crenata* fiber after delignification and xylanase degradation

4.1 Introduction

Wood cell walls are mainly composed of cellulose, hemicelluloses, and lignins. The mechanical properties of cell walls, therefore, are dependent on the distribution and molecular properties of these components. Hemicelluloses are the second most abundant material following cellulose in hardwoods. Xylan, in particular, accounts for 20 to 30% of cell wall materials in hardwoods (Fengel and Wegener 1989). Therefore, the distribution and molecular properties of xylan make an important contribution to the properties of hardwood cell walls. The distribution of xylan, however, is not as well known as that of cellulose and lignin.

In the previous Chapters, localization of xylan in differentiating xylem was observed by immunogold labeling. The results suggest that xylan located only in the secondary wall of xylem elements. In this Chapter, xylan localization was examined by field emission scanning electron microscopy (FESEM) and transmission electron microscopy (TEM) with selective extraction. *Fagus crenata* sections were mildly delignified without loss of hemicellulose and treated with xylanase to selectively remove xylan.

The acid chlorite delignification method of Wise et al. (1946) has long been used for holocellulose preparation. It is not an ideal procedure for ultrastructural observation, however, because delignification is performed at a high temperature. Maekawa and Koshijima (1983) evaluated several delignification procedures and concluded that the use of acetate buffer as a reaction medium in the Wise method promotes the delignification process and reduces the loss of carbohydrates. In addition, they concluded that the delignification method of Klaudiz (1957), delignification at 35 to 40°C for a longer period, is a comparable procedure when attempting to minimize the loss of carbohydrate. From an anatomic point of view, the method of Klaudiz should be adequate because the reaction proceeds at a relatively low temperature. The extracted materials and the residual sections were chemically analyzed.

The changes in the cell wall structure observed by TEM and FESEM revealed the

role of lignin and xylan in the cell wall. The combined use of the enzymatic and immunolabeling methods confirmed the localization. Moreover, extensive swelling of the secondary wall after xylanase degradation is discussed. This phenomenon suggests that xylan acts as a cementing material for the lamellated structure of cellulose microfibrils in the secondary wall.

4.2 Materials and Methods

4.2.1 Plant material

During the active growth period, small blocks (5 x 5 x 15 mm) containing differentiating xylem were taken from a living *Fagus crenata* Blume grown in the Kamigamo Experimental Forest (Kyoto, Japan). Blocks were fixed and stored in 3% glutaraldehyde in 0.1 M phosphate buffer (pH 7.2) at 4°C .

The specimen blocks were sectioned in the radial plane at a thickness of 100 μm using a sliding microtome. These sections were used for the following extraction procedure (delignification and xylanase degradation).

4.2.2 Sodium chlorite delignification

Delignification was performed according to Klaudiz (1957) with minor modifications. For chemical analysis, 1 g of extracted, oven-dried sections was weighed. For TEM and FESEM observation, approximately 1 g of never-dried sections was used. Sections were treated with 50 ml of 8% $NaClO_2$ in 1.5% acetic acid at 40°C for 24 to 96 h. After treatment, the sections were washed several times with distilled water.

4.2.3 Lignin analysis

The lignin content of the lignin extracted sections was determined using the sulfuric acid method. Klason lignin (acid-insoluble lignin) was determined according to Effland

(1977). Klason lignin was calculated as the percent of the extracted, oven-dried sample. The wood sections (200 mg) were dissolved in 1 ml of 72% sulfuric acid (30°C, 1 h). Thereafter, the specimens were diluted using 28 ml of distilled water and placed in an autoclave for 1 h at 120°C. While keeping the solution hot, the lignin was filtered off through a 1G4 filter.

Theacid-soluble lignin content was determined according to Maekawa et al. (1989). The absorbance of the filtrate was measured at 205 nm. The acid-soluble lignin content in the filtrate was calculated using 110 ($Lg^{-1}cm^{-1}$) as the absorptivity of the lignin. The filtrate after acid hydrolysis (8.7 ml) was used for analysis of the neutral monosaccharides as described in following section.

4.2.4 Xylanase degradation

Following 72 h of sodium chlorite delignification, parts of sections were incubated with xylanase from *Trichoderma viride* (X-3876, Sigma Chemical Co., St. Louis, MO). Dry delignified sections (100 mg) were weighed and incubated with 25 U xylanase in 10 ml of 0.1 M acetate buffer (pH 4.5) for 1 week. As a control, dry delignified sections (100 mg) were incubated in the same acetate buffer without xylanase for 1 week. After incubation, sections were separated from enzyme hydrolysate solution by centrifugation.

Degradation was determined by two methods: measurement of the visible and UV spectra of the xylanase hydrolysate solution and neutral monosaccharide analysis of the xylanase hydrolysate solution and the residual sections. The visible and UV spectra of the xylanase hydrolysate solution were determined with a spectrophotometer (UV-1600, Shimadzu, Kyoto, Japan). Thereafter, 0.3 ml of 72% sulfuric acid was added to the xylanase hydrolysate solution (8.4 ml) and the mixture was autoclaved for 1 h at 120°C. The solution obtained (8.7 ml) was used for neutral monosaccharide analysis as described in the following section. The xylanase-treated sections (30 mg) were weighed and dissolved in 0.3 ml 72% sulfuric acid (30°C, 1 h). Thereafter, the specimens were diluted in 8.4 ml distilled water and placed in an autoclave for 1 h at 120 °C. The

solution was collected by filtration through a 1G4 filter. The filtrate (8.7ml) was used for neutral monosaccharide analysis as described in the following section.

For microscopic observation, approximately 100 mg of delignified sections which have not been dried was incubated with 12.5 U xylanase in 10 ml of 0.1 M acetate buffer (pH 4.5) for 1 week. As a control, some sections were treated with the same acetate buffer without xylanase. The enzyme reaction was stopped by thoroughly washing with distilled water. The residual sections were used for TEM and FESEM specimen preparation described below.

4.2.5 Neutral monosaccharide analysis

Myo-inositol (0.5 ml, 20 mg/ml) was added to the sample solution (8.7 ml) as an internal standard. Thereafter, the pH of the solution was adjusted to 5.5 with saturated barium hydroxide. The solutions were centrifuged and the supernatant was collected. Sodium borohydride (20 mg) was added to the supernatant. The reaction mixture was maintained at room temperature overnight. The reduction reaction was stopped by dropwise addition of glacial acetic acid until the evolution of hydrogen gas ceased. Then, the reaction mixture was dried by evaporation at 50°C. To remove the volatile methyl borate esters, 10 ml ethanol was added to the mixture and evaporated at 50 °C three times. Sulfuric acid (0.1 ml) was added to the reaction mixture followed by the addition of 2 ml acetic anhydride. The resultant solution was mixed thoroughly and maintained at 60 °C for 1 h. After the addition of 20 ml of water, alditol acetates were extracted with 15 ml of ethyl acetate, followed by rinse with distilled water, saturated sodium hydrogen acetate, and saturated sodium chloride. The extracts were dried over sodium sulfate and evaporated to dryness. The alditol acetates were dissolved in acetone and quantitatively determined by gas chromatography on a fused-silica capillary column (SP-2330, 0.25 mm X 15 m, SUPELCO).

4.2.6 TEM observation

Sections were dehydrated through a graded ethanol series and embedded in epoxy resin. Ultrathin sections of the epoxy-embedded samples were cut transversely with an ultramicrotome (Ultracut E, Reichert-Jung). Some sections were immunolabeled with anti-xylan antiserum as described in Chapter 2. Ultrathin sections with or without immunolabeling were stained with 2% aqueous uranyl acetate and Reynolds' lead citrate. The ultrathin sections were observed with a TEM (JEM-1220, JEOL) at 100 kV.

4.2.7 FESEM observation

Sections were postfixed with 2% osmium tetroxide for 2 h at room temperature. Thereafter they were dehydrated through a graded ethanol series and dried with a critical point dryer (HCP-2, Hitachi) with liquid CO_2 as the drying agent. Dried sections were coated with approximately 1 nm thick platinum-carbon by rotary shadowing at a 60° with a freeze etching apparatus (JFD-9010, JEOL). Sections were examined with a FESEM (S-4500, Hitachi) at an accelerating voltage of 1.5 kV and 3 to 5 mm of working distance.

4.3 Results

4.3.1 Lignin content of delignified sections

Yield and lignin content of delignified sections are shown in Table 4.1. Prolonged sodium chlorite treatment decreased Klason lignin content. No Klason lignin was detected in the sections treated for more than 48 h. The acid-soluble lignin content in the sodium chlorite-treated sections was higher than that in control sections.

4.3.2 Estimation of xylanase degradation

The visible and UV spectra of the xylanase hydrolysate solution are shown in Fig. 4.1. Both xylanase hydrolysate solution and acetate buffer solution had UV absorption. There was no visible light absorption. The UV absorption of xylanase hydrolysate was slightly higher than that of acetate buffer solution. Neutral monosaccharide composition of xylanase-treated sections is shown in Table 4.2. Xylanase-treated sections had a low xylose content. Neutral monosaccharides of the xylanase hydrolysate solution are shown in Table 4.3. Xylanase hydrolysate contained not only xylose but also other monosaccharides. The amount of other monosaccharides in the xylanase hydrolysate, i.e., arabinose, mannose, galactose, and glucose, however, was the same as that in acetate buffer (control).

4.3.3 TEM observation

Figure 4.2 shows a transverse view of a mature fiber. The middle lamella and primary wall were heavily contrasted in untreated sections and the three-layered secondary wall (S_1, S_2 and S_3) was weakly stained (Fig. 4.2A). The shape of the secondary wall did not change after delignification, and materials were extracted from the cell corner middle lamellae showing a reticular structure, while the primary wall remained heavily contrasted (Fig. 4.2B). The secondary wall was not affected by the delignification process with regard to shape and stainability. Xylanase treatment following delignification markedly affected secondary wall structure (Fig. 4.2C). The fiber cell wall changed to a rounded shape and the secondary wall was inwardly swollen. No fibrillar structure was observed in cell corner middle lamella. Control specimens treated with only acetate buffer had no structural changes in the secondary wall (Fig. 4.2D). The cell corner middle lamellae, however, was electron transparent and the primary wall was lightly stained.

Figure 4.3 illustrates the immunolocalization of xylan in the fiber cell wall. Gold

particles were observed not only in the S_1-S_2 transition zone but also in the S_2 and S_3 layers of control sections (Fig. 4.3A) and delignified sections (Fig. 4.3B). There were no particles observed in the compound middle lamellae. In xylanase-degraded sections, gold particles were seldom observed in the fiber cell wall (Fig. 4.3C).

4.3.4 FESEM observation

Radial sections containing mature xylem were observed by FESEM. The two adjacent fibers were extensively separated from each other in the xylanase-degraded sections (Fig. 4.4C), whereas this separation was not as extensive in either the control sections (Fig. 4.4A) or the delignified sections (Fig. 4.4B). The separated surface always appeared in either of two adjacent fibers and the interface between the S_1 layer and the primary wall (Fig. 4.4D). In xylanase-degraded sections, the S_3 layer swelled extensively (Fig. 4.5A). Macrofibrils were compressed in the direction of their molecular axis, forming waves along the longitudinal axis of the fiber cell (Fig. 4.5B).

4.4 Discussion

4.4.1 Delignification

Klason lignin was not detected in the sections treated for more than 48 h. The acid-soluble lignin content in the sodium chlorite-treated sections was higher than that in the control sections. Lignin molecules were degraded into small fragments that were solubilized in the acid solution. The content of acid soluble lignin decreased as treatment time increased. To decrease the lignin content, delignification should be performed for a longer period. A longer period of delignification, however, decreased the yield of the specimen, which indicates an increased loss of carbohydrate (Table 4.1). In the present study, the delignification period was 72 h, a compromise between a low lignin content

and a low loss of carbohydrate.

4.4.2 Specificity of xylanase degradation

In the present Chapter, xylanase was used as a selective extracting reagent for xylan. To examine the specificity of xylanase degradation, enzyme hydrolysate and enzyme-degraded sections were chemically analyzed. The UV spectra of enzyme hydrolysate revealed that some UV-absorbing materials were extracted during xylanase incubation (Fig. 4.1). Acetate buffer without xylanase, however, also extracted some UV-absorbing materials (Fig. 4.1). Xylanase hydrolysate contained not only xylose, but other monosaccharides as well, i.e. , arabinose, mannose, galactose, and glucose (Table 4.3). Acetate buffer after incubation also contained almost the same amount of these monosaccharides but less xylose (Table 4.3). These results suggest that some UV-absorbing materials and non-xylose neutral monosaccharides were extracted by acetate buffer alone.

Xylanase treatment affected the secondary wall as well as primary wall and cell corner middle lamellae (Fig. 4.2C). On the other hand, acetate buffer induced morphologic changes in the primary wall and cell corner middle lamella but not in the secondary wall (Fig. 4.2D). Therefore, xylanase rather than acetate buffer induced morphologic changes in the secondary wall.

The author concluded that the specificity of xylanase treatment was relatively high in the secondary wall. There was no ultrastructural difference observed in the secondary wall under FESEM, regardless of acetate buffer treatment (data not shown). Delignified sections contain only acid-soluble lignin but no Klason lignin (Table 4.1). After sodium chlorite treatment, xylanase degraded the entire secondary wall, which was located in the middle of a 100-μm thick radial section (Fig. 4.2C, 4.3C), although this enzyme could not degrade lignified cell walls (data not shown). Therefore, the fibers in the 100-μm thick section had been entirely delignified by sodium chlorite treatment.

4.4.3 Xylan localization

Previous immunogold labeling studies revealed that xylan is distributed exclusively in the secondary wall (Chapter 2, 3). In this Chapter, the delignified section was observed by the same technique. In the delignified sections, the distribution and density of labeling was almost the same as in control sections (Fig. 4.3B). This result suggests that lignin did not mask the xylan epitope. In softwood, lignin deposition inhibited access of the anti-glucomannan antiserum to glucomannan epitope (Maeda et al. 2000). The difference in epitope masking behavior might reflect a difference in the lignin composition or the hemicellulose-lignin relation between hardwoods and softwoods.

After xylanase degradation, structural changes were observed in cell corner middle lamellae as well as in the secondary wall (Fig. 4.2C, 4.3C). Xylanase, however, seems to degrade only the secondary wall, because an acetate buffer, used as a solvent for xylanase, extracts phenolic materials and some polysaccharides except xylan from both compound middle lamellae and cell corner middle lamellae (Fig. 4.1, 4.2D). Immunogold labeling of anti-xylan antiserum was not observed in xylanase-degraded sections (Fig. 4.3C), though xylanase-degraded sections still contained 13.6% xylose (Table 4.1). This finding suggests that the epitope in the xylan molecule was changed by xylanase degradation and the entire secondary wall was affected.

4.4.4 Swelling of the secondary wall induced by xylanase degradation

Xylanase degradation caused extensive swelling of the secondary wall. The fiber cell wall had a rounded shape in a transverse section after xylanase degradation (Fig. 4.2C), whereas it had an angular shape in controls and delignified specimens (Fig. 4.2A, 4.2B). Swelling progressed inwardly but not outwardly, as indicated by a decrease in the lumen and an enlargement of the cell corner region (Fig. 4.2C). Extensive swelling of the secondary wall was also observed using FESEM. Two adjacent fibers were extensively separated from each other in xylanase-degraded sections (Fig. 4.4C), whereas

this separation was not as extensive in controls and delignified sections (Fig. 4.4A, 4.4B). The separated surfaces always appeared on either side of two adjacent fibers, and the interface between the S_1 layer and the primary wall (Fig. 4.4D). This separation seemed to be induced by mechanical force tearing the two cell walls apart. Macrofibrils in the S_3 layer were compressed in the direction of their molecular axis, forming waves along the longitudinal axis of the fiber cell (Fig. 4.5). Cotê et al. (1969) observed similar swelling of the secondary wall in delignified aspen wood fibers. The delignification method used in their study was so severe that hemicellulose might have eluted from the cell wall.

Xylan appears to act as a cementing material for the lamellated structure of cellulose microfibrils in the secondary wall. In differentiating tracheids of *Cryptomeria japonica* D. Don, hemicelluloses deposit in the expanded gaps between cellulose microfibrils, which are generated by high turgor pressure at night (Yoshida et al. 2000). If hemicelluloses, especially xylan, are deposited similarly in the fiber cell wall of hardwoods, internal stress within cell wall would be generated as follows. The fiber cell wall is stretched outwardly by high turgor pressure. The gaps between cellulose microfibrils or cellulose lamellae are widened and xylan deposits in them. Xylan prevents cell wall shrinkage and therefore compressive stresses are generated in a transverse direction between cellulose microfibrils. The secondary wall swelling observed in the present study might be due to the release of the compressive stresses caused by xylan removal.

4.5 Abstract

Delignified and/or xylanase-treated secondary walls of *Fagus crenata* Blume fibers were examined by TEM and FESEM. Radial sections (100 μm thick) of *Fagus crenata* Blume were delignified in mild conditions and degraded by xylanase. Lignin contents

and monosaccharide composition of the extracted materials and the residual sections were determined. The data of chemical analysis suggested that sections were delignified with low loss of carbohydrates and xylanase selectively degraded xylan.

Extraction occurred throughout radial sections, shown by micrographs taken of the fiber cell wall located in the middle of thick sections. Immunogold labeling by anti-xylan antiserum was observed in the secondary wall of controls and delignified sections. No labeling, however, was observed in the xylanase-degraded sections. Xylanase degradation caused extensive swelling of the secondary wall. A transverse view of the fiber cell wall revealed a rounded shape after xylanase degradation, and an angular shape in controls and delignified sections. Swelling caused separation of the two adjacent fiber cell walls. The secondary wall swelling might be due to the release of compressive stresses caused by xylanase degradation of xylan. Xylan might act as a cementing material for the lamellated structure of cellulose microfibrils in the secondary wall.

Table 4.1 Yield and lignin content of delignified sections

	Delignification time (hours)				
	0	24	48	72	96
Yield (%)	100	83.1	78.6	75.3	74.0
Klason lignin (%)	18.2	2.1	0.0	0.0	0.0
Acid-soluble lignin (%)	2.6	7.1	6.4	5.7	5.2
Total lignin (%)	20.8	9.2	6.4	5.7	5.2
(% on original section)	(20.8)	(7.6)	(5.0)	(4.3)	(3.8)

Table 4.2 Neutral monosaccharide composition of sections

	Relative amount of neutral monosaccharides (%)				
	Ara	Xyl	Man	Gal	Glc
Untreated	0.8	26.1	2.1	1.2	69.9
Delignified	0.6	28.4	2.1	0.8	68.1
Delignified/buffer treated	0.8	28.2	2.4	0.7	68.0
Delignified/xylanase treated	0.5	13.6	2.7	0.7	82.5

Table 4.3 Neutral monosaccharides derived from sections treated with acetate buffer with or without xylanase

	Neutral monosaccharides (mg/100 mg of delignified section)				
	Ara	Xyl	Man	Gal	Glc
Buffer (Control)	0.1	2.3	0.1	0.1	2.1
Xylanase	0.4	17.2	0.1	0.1	3.2

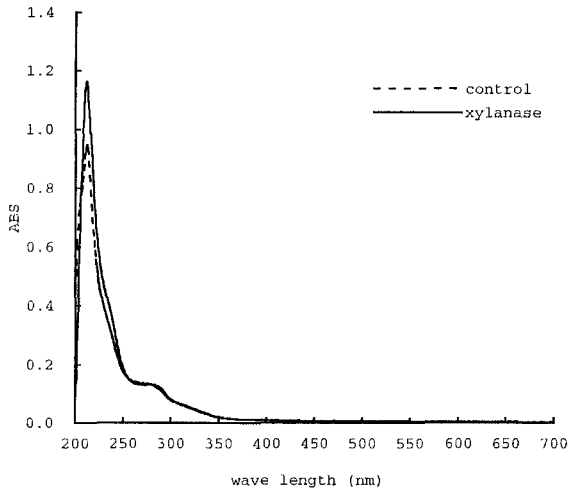

Fig. 4.1

The visible and UV spectra of the xylanase hydrolysate. The solid line indicates the spectrum of xylanase hydrolysate. The broken line indicates the spectrum of acetate buffer solution (control).

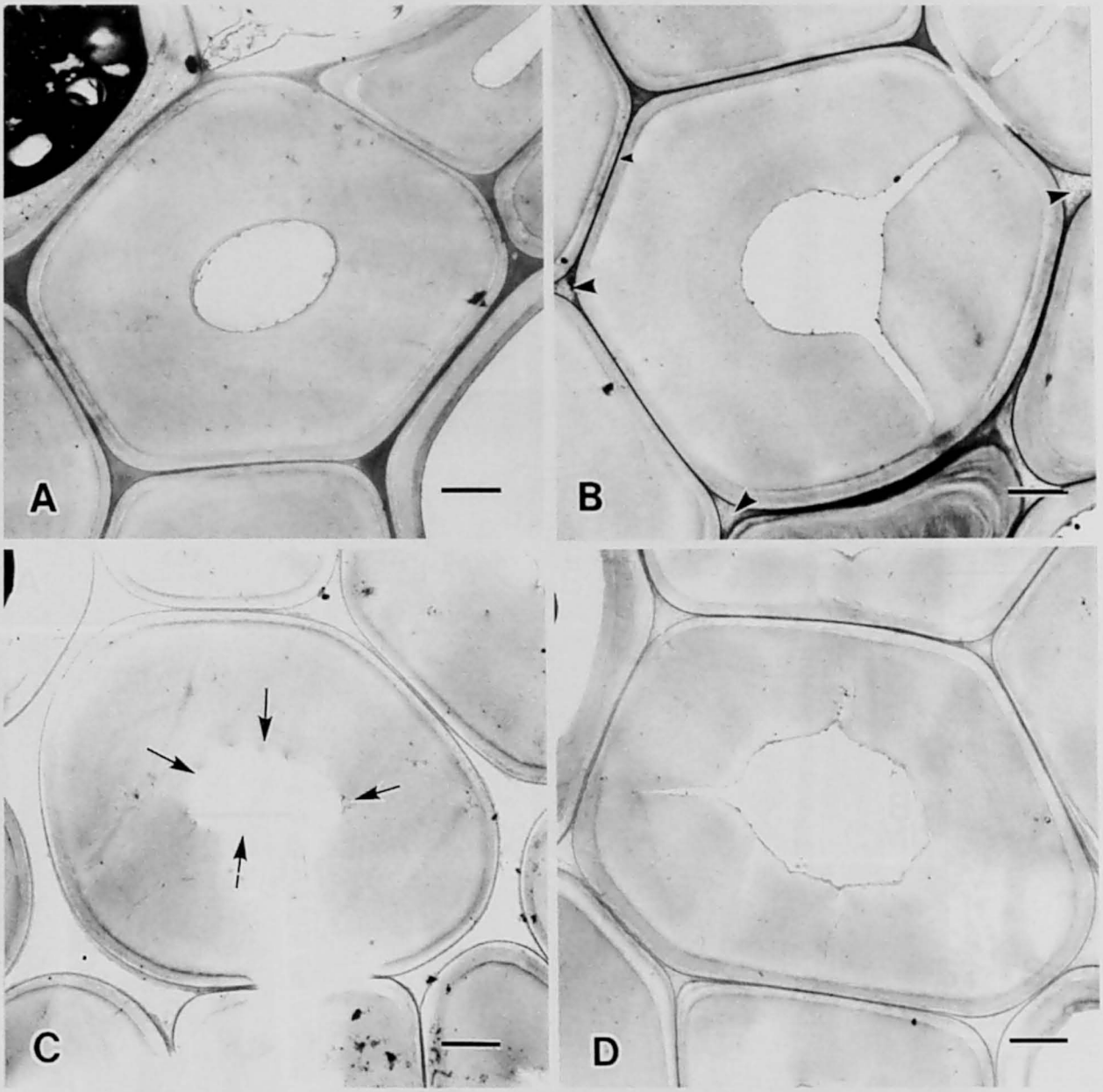

Fig. 4.2

TEM observation of transversely sectioned mature fiber. **A** Control section. Primary wall and middle lamellae cell corner were heavily contrasted. **B** Delignified section. Materials were extracted from the middle lamellae cell corner showing a reticular structure (arrowheads). The primary wall remained heavily contrasted. **C** Delignified and xylanase-treated section. Secondary wall expanded toward cell lumen (arrows). Primary wall was lightly stained. No fibrilar structure was observed in middle lamellae cell corner. **D** Delignified and acetate buffer treated section. No structural change was observed in the secondary wall. Middle lamellae cell corners, however, were electron translucent and primary walls were lightly stained. Bars = 2 μm.

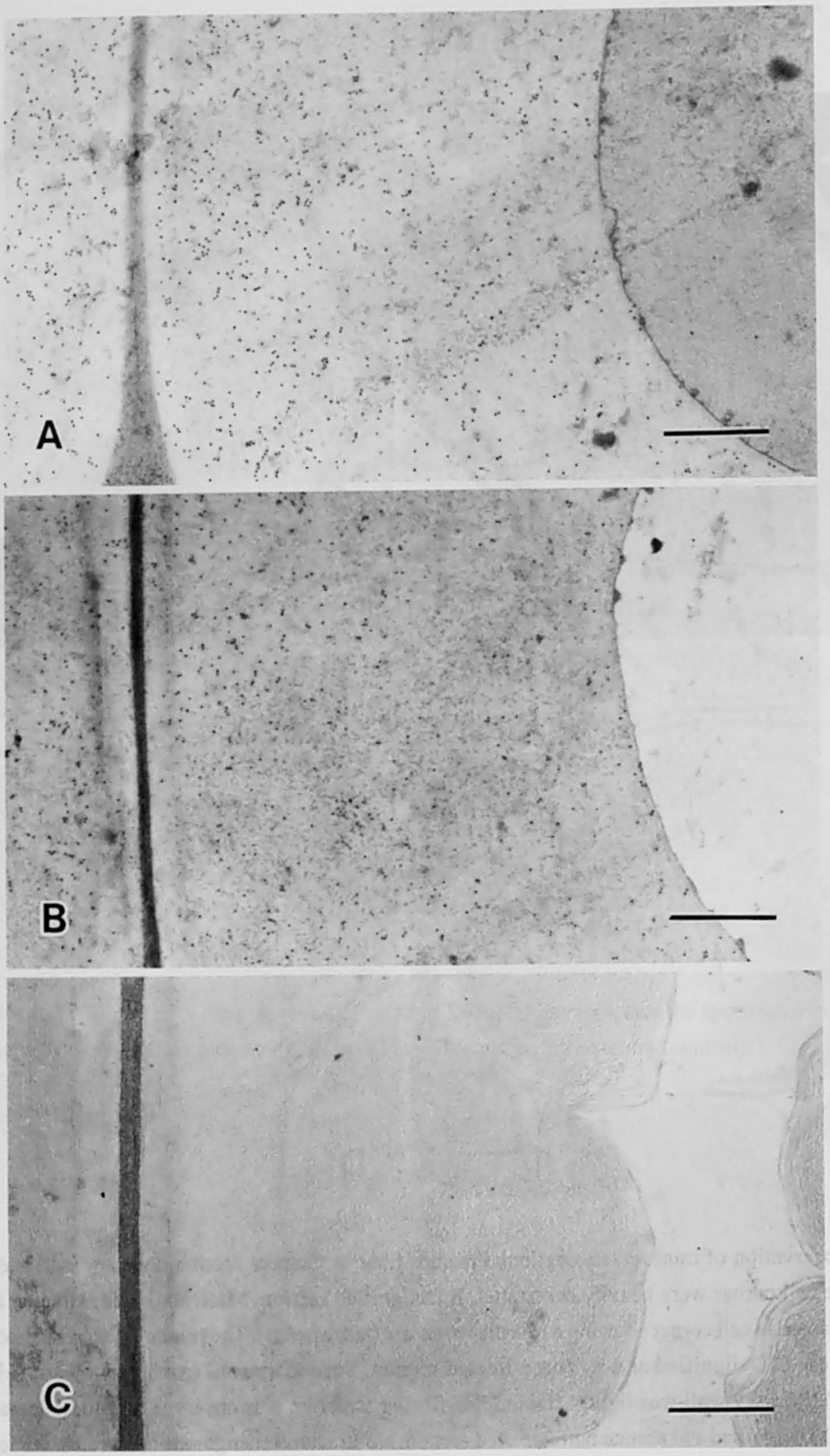

Figs. 4.3

Anti-xylan immunogold labeling of a mature fiber. **A** Control section. Gold labeling was observed only in the secondary wall. Bar = 1 μm. **B** Delignified section. Gold labeling was observed only in the secondary wall and the labeling density was almost same as the control section. Bar = 1 μm. **C** Delignified and xylanase-treated section. Gold particles were rarely observed. Bar = 1 μm.

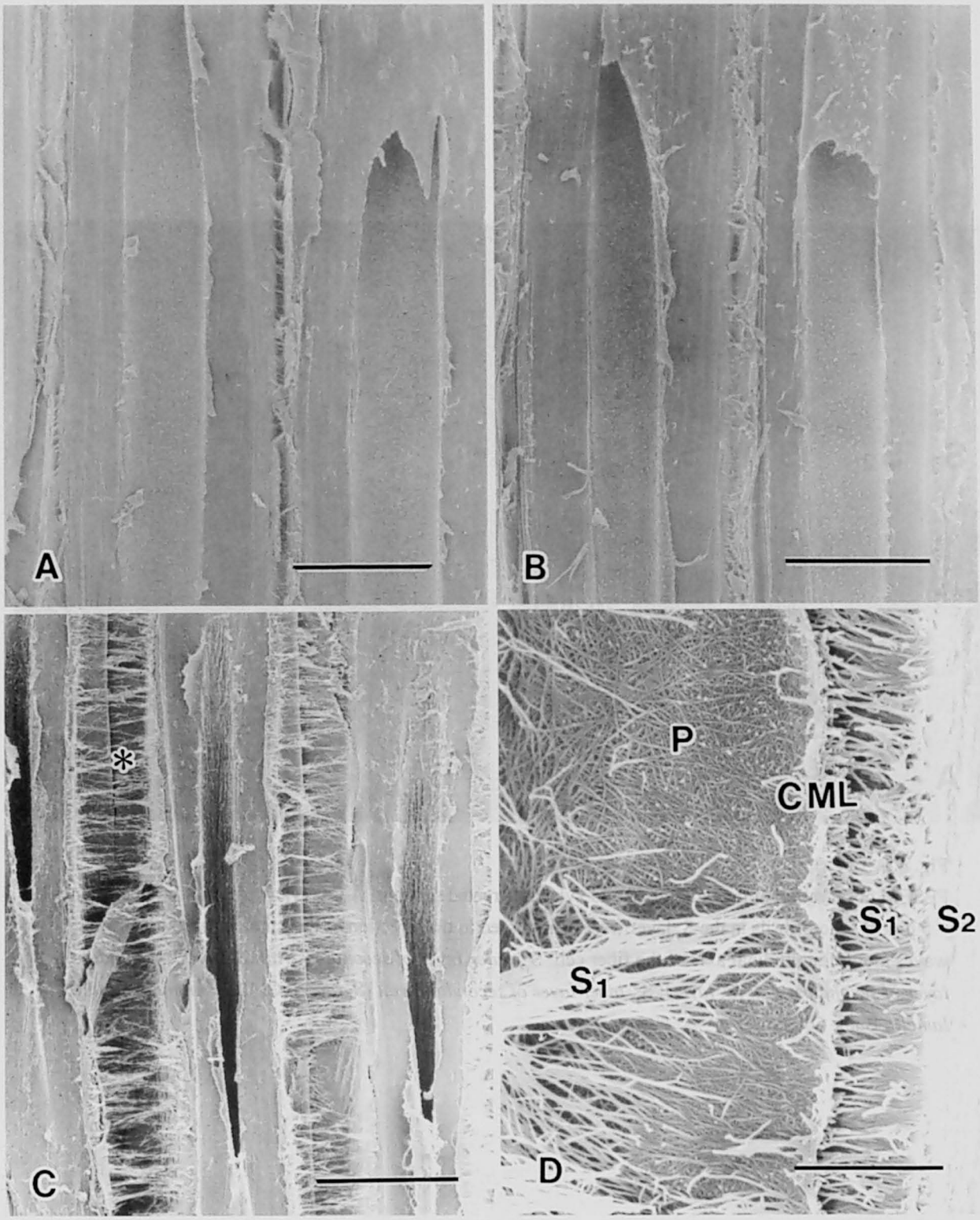

Fig. 4.4

FESEM observation of a mature fiber. **A** Control section. Two adjacent mature fibers were observed. The compound middle lamella was slightly separated by sectioning. Bar = 10 μm. **B** Delignified section. The compound middle lamella was slightly separated by sectioning as well as in the control section. Bar = 10 μm. **C** Delignified and xylanase-treated section. The compound middle lamella was extensively separated and the S_1 layer was torn apart (asterisk). Bar = 10 μm. **D** Delignified and xylanase-treated section. High magnification of the asterisk in **C**. The separated surface always appeared on either side of two adjacent fibers, the interface between the S_1 layer and the primary wall. CML, *compound middle lamella*; P, *prymary wall*; S_1, *outer layer of secondary wall*; S_2, *middle layer of secondary wall*. Bar = 1 μm.

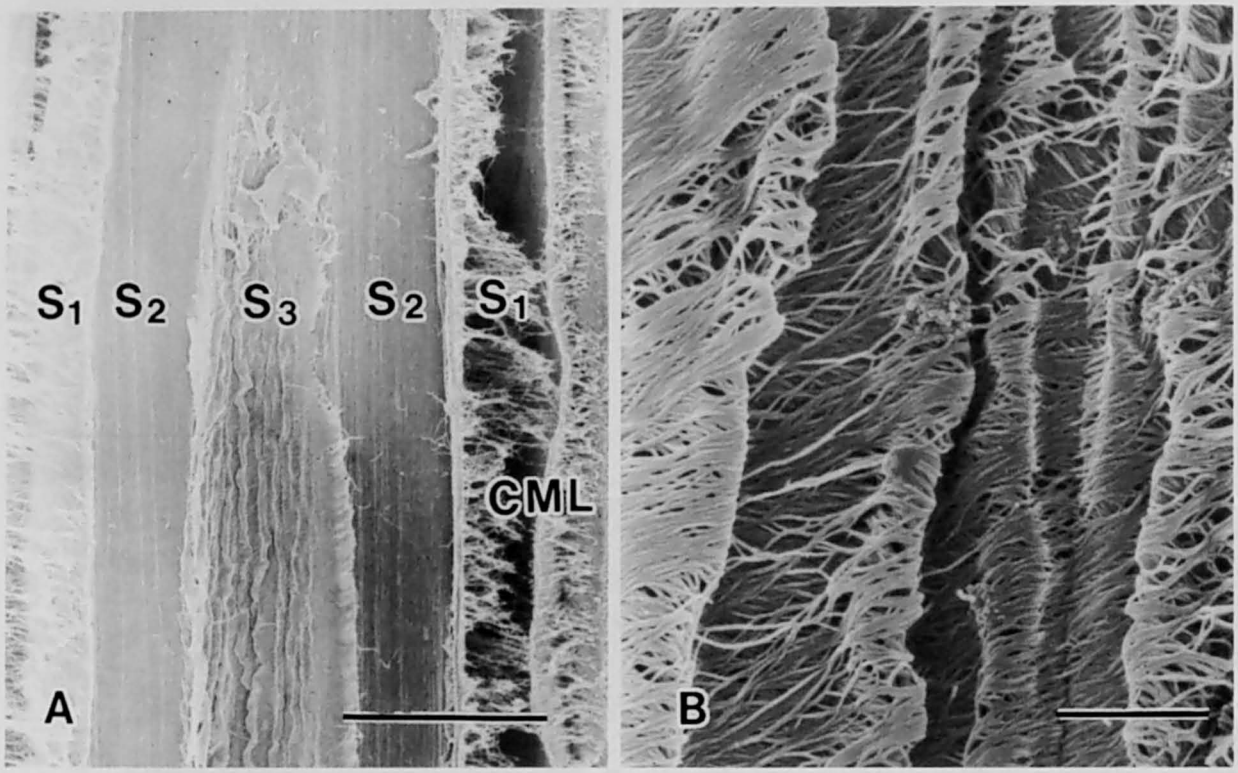

Fig. 4.5

FESEM observation of the delignified and xylanase-treated sections. **A** Overview of a mature fiber. Bar = 5 μm. **B** Macrofibrils in the S_3 layer were compressed in the direction of their molecular axis, forming waves along longitudinal axis of the fiber cell. S_1, *outer layer of secondary wall (S_1 layer)*; S_2, *middle layer of secondary wall (S_2 layer)*; S_3, *inner layer of secondary wall (S_3 layer)*; CML, *compound middle lamella* Bar = 500 nm.

Chapter 5

Deposition of xylan on *Fagus crenata* fiber observed by field emission scanning electron microscpy with selective extraction

5.1 Introduction

In the previous Chapters, the immunolocalization of xylan in the differentiating xylem of *Fagus crenata* was examined. Xylan was exclusively located in the secondary wall of xylem elements and gradually increased during the course of secondary wall formation (Chapter 2). The increase of xylan in the differentiating secondary wall was supported by immuno-scanning electron microscopy (Chapter 3). Macrofibrils in newly formed secondary walls as well as in mature secondary walls were labeled with anti-xylan antiserum. The intensity of labeling was greater in mature secondary walls than in differentiating cell walls, suggesting that deposition of xylan into the cell wall occurs continuously after macrofibril deposition. The diameter of the macrofibrils increased during the course of secondary wall formation. The increase in the diameter of the macrofibrils might be due to successive xylan deposition.

Macrofibrils observed by FESEM are not composed of pure cellulose, but are groups of cellulose microfibrils coated with xylan. Xylan, however, is not the only molecule that causes macrofibril thickening. Lignin also deposits around macrofibrils and contributes to the thickening of the macrofibrils. When mature cell walls were observed by FESEM, macrofibrils were not apparent. In mature cell walls, lignin might cover other cell wall components and contribute to cell wall consolidation. Therefore, lignin removal without loss of other cell wall components is necessary for visualization of macrofibrils and hemicellulose by FESEM.

In this Chapter, *Fagus crenata* sections mildly delignified as described in Chapter 4 were observed by FESEM. Delignified sections were treated with xylanase to remove xylan. FESEM observation of these sections revealed the spatial relations of cellulose microfibrils, xylan, and lignin (Awano et al. 2002).

5.2 Materials and Methods

5.2.1 Plant material

During the active growth period, small blocks (5 x 5 x 15 mm) containing differentiating xylem were taken from a living *Fagus crenata* tree grown in the Kamigamo Experimental Forest (Kyoto, Japan). Blocks were fixed and stored in 3% glutaraldehyde in 0.1 M phosphate buffer (pH 7.2) at 4°C. Specimen blocks, stored as described previously, were sectioned in the radial plane at a thickness of 100 μm using a sliding microtome.

5.2.2 Delignification and xylanase degradation

The sections were delignified and degraded with xylanase as described in Chapter 4.

5.2.3 FESEM observation

Sections were postfixed with 2% osmium tetroxide for 2 h at room temperature. Thereafter they were dehydrated through a graded ethanol series and dried using a critical point dryer (HCP-2; Hitachi, Tokyo, Japan) with liquid CO_2 as the drying agent. Dried sections were coated with approximately 1 nm thick platinum/carbon by rotary shadowing at a 60° angle using a freeze etching apparatus (JFD-9010; JEOL, Tokyo, Japan). Sections were examined with a FESEM (S-4500; Hitachi, Tokyo, Japan) at an accelerating voltage of 1.5 kV and 3 to 5 mm of working distance.

5.3 Results

5.3.1 FESEM observation of control sections

The S_2-forming fibers were observed by FESEM. Macrofibrils on the innermost surface of the cell wall were highly oriented to the cell axis (Fig. 5.1A). Although

macrofibrils were clearly visible near the innermost surface, they were gradually indiscernible toward the outer part of the secondary wall (Fig. 5.4). No fibrillar structure was visible and many warts were observed on the inner surface of mature fiber cell walls (Fig. 5.2A). Macrofibrils were not visible in the sliced surface of the secondary wall (Fig. 5.3A).

5.3.2 FESEM observation of delignified sections

Macrofibrils on the innermost surface of the secondary wall in the S_2-forming fibers were clearly visible (Fig. 5.1B). On the obliquely-sliced surface of the S_2-forming fiber cell wall, macrofibrils at the outer part of the secondary wall had many globular substances on them, while the inner part of secondary wall had a smooth surface (Fig. 5.5). When the mature fiber was observed from the lumen side, macrofibrils were visible and many globular substances were located on the macrofibrils (Fig. 5.2B). The size of the globular substance was almost the same as the width of the macrofibrils. Warts were clearly observed (Fig. 5.2B). Macrofibrils on the sliced surface of the secondary wall had many globular substances on their surface (Fig. 5.3B).

5.3.3 FESEM observation of delignified and xylanase-treated sections

In the S_2-forming fibers, macrofibrils on the innermost surface of the secondary wall were clearly visible (Fig. 5.1C). The width and appearance of the macrofibrils were almost the same as that of the control and delignified sections. When the mature fiber was observed from the lumen side, macrofibrils were visible, but there were no globular substances (Fig. 5.2C). There were no warts observed (Fig. 5.2C). On the sliced surface of the secondary wall, macrofibrils were clearly visible and there was no globular substance on the macrofibrils (Fig. 5.3C).

5.4 Discussion

5.4.1 Secondary wall of the differentiating fiber

The innermost surface of the differentiating secondary walls can be regarded as newly formed cell walls. Macrofibrils were clearly visible in the control sections and were highly oriented to the cell axis in the S_2 layer (Fig. 5.1A). After delignification, macrofibrils retained almost the same diameter and had the same appearance as controls (Fig. 5.1B), indicating that lignin deposition had not occurred in the innermost surface of the cell wall. Xylanase treatment did not change the diameter or appearance of the macrofibrils (Fig. 5.1C). Macrofibrils on the innermost surface of cell walls, however, are immunolabeling with anti-xylan antiserum (Chapter 2). Therefore, they were coated with a very thin layer of xylan that could not be resolved by FESEM.

The outer part of the differentiating secondary wall is in the advanced stage of cell wall formation. Although macrofibrils were clearly visible near the inner region, they were gradually indiscernible toward the outer part of the secondary wall (Fig. 5.4). After delignification of the developing secondary walls, macrofibrils with many globular substances were visible in the outer part of the wall, while the macrofibrils were observed on the smooth surface in the inner part of the wall (Fig. 5.5). This finding suggests that lignin deposition occurs on the outer part of the cell wall and does not start in the inner part. The globular substances on the macrofibrils disappeared following xylanase treatment (Fig. 5.3C), indicating that these substances are xylan. Therefore, xylan not only covers the newly-deposited macrofibrils in the inner part of the secondary walls, but also deposits heavily on macrofibrils in the outer part of the secondary wall. Various stages of cell wall formation were simultaneously observed in obliquely-sliced secondary walls. The gradual increases in the globular substances toward the outer part of secondary wall (Fig. 5.5) suggests that larger amounts of xylan penetrated into the cell wall and continuously deposited on macrofibrils.

5.4.2 Secondary wall of mature fiber

The fiber cell walls of *Fagus crenata* Blume have a warty layer (Harada 1962). Many warts were clearly observed on the innermost surface (Fig. 5.2A). This layer did not disappear following xylanase treatment without delignification (data not shown). Therefore, this layer might be covered by lignin or other materials. Warts remained after delignification (Fig. 5.2B), but completely disappeared after xylanase treatment (Fig. 5.2C), indicating that warts are mainly composed of xylan. No fibrillar structure was visible on the innermost surface of the fiber cell wall because a warty layer covered the surface (Fig. 5.2A). In delignified sections, macrofibrils with many globular substances were visible (Fig. 5.2B). The size of the globular substance was almost the same as the width of the macrofibrils. Following xylanase treatment, the globular substance disappeared and therefore the macrofibrils had a smooth surface (Fig. 5.2C). This indicates that these globular substances on the macrofibrils are xylan.

Macrofibrils in the mature S_2 layer were not visible in control sections (Fig. 5.3A). In delignified sections, macrofibrils with many globular substances on their surface were clearly visible (Fig. 3B). Following xylanase treatment, the macrofibrils had a smooth surface, indicating that the globular substance is xylan (Fig. 5.3C).

5.4.3 Mechanism of secondary wall assembly

The author proposes the following mechanism for secondary wall assembly. There are two phases of xylan deposition. First, xylan coats the surface of cellulose macrofibrils that have just been released into the innermost surface of the cell wall. This thin layer of xylan could not be resolved by FESEM, but was immunolabelied with anti-xylan antiserum (Chapter 3). Second, large amounts of xylan penetrates into the cell wall because there is no room for xylan to coat the cellulose macrofibril surface. This type of xylan accumulates on the macrofibrils and has a globular appearance. These globular substances, however, were not observed in the control sections, which suggests that

lignin deposition occurs simultaneously with xylan penetration.

5.5 Abstract

Delignified and/or xylanase-treated secondary walls of *Fagus crenata* Blume fibers were examined by field emission scanning electron microscopy (FESEM). Macrofibrils with a smooth surface were visible in the innermost surface of the differentiating fiber secondary wall. There was no ultrastructural difference between control and delignified sections, indicating that lignin deposition had not started in the innermost surface of the cell wall. There was no ultrastructural difference between control and xylanase-treated sections.

Macrofibrils on the outer part of the differentiating secondary wall had globular substances in delignified sections. These globular substances disappeared following xylanase treatment, indicating that these globules are xylan. The globular substances were not visible near the inner part of the differentiating secondary wall but gradually increased toward the outer part of the secondary wall, indicating that xylan penetrated into the cell wall and continuously accumulated on the macrofibrils.

Mature fiber secondary walls were also examined by FESEM. Macrofibrils were not apparent in the secondary wall in control specimens. Macrofibrils with many globular substances were observed in the delignified specimens. Following xylanase treatment, the macrofibrils had a smooth surface without any globules, indicating that the globular substance is xylan.

These results suggest that macrofibrils on the innermost surface of the secondary wall are coated with a thin layer of xylan and successive deposition of xylan into the cell wall increases macrofibril diameter. The large amounts of xylan that accumulated on macrofibrils appear globular, but are covered with lignin after they are deposited.

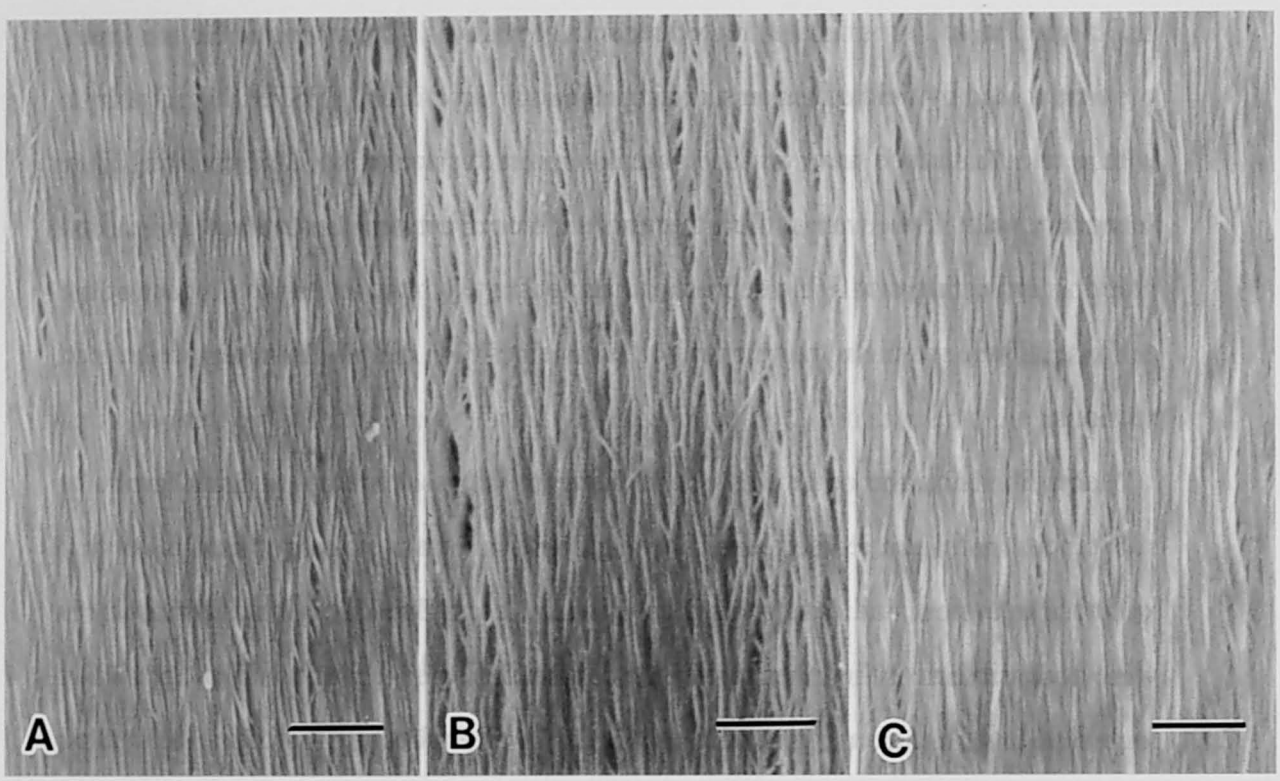

Fig. 5.1

FESEM observation of the innermost surface of the S_2-forming fiber secondary wall. **A** Control section. Macrofibrils were clearly visible. **B** Delignified section. Macrofibrils had almost the same diameter and appearance as the control sections. **C** Delignified and xylanase-treated section. No structural change was observed. Bars = 200 nm

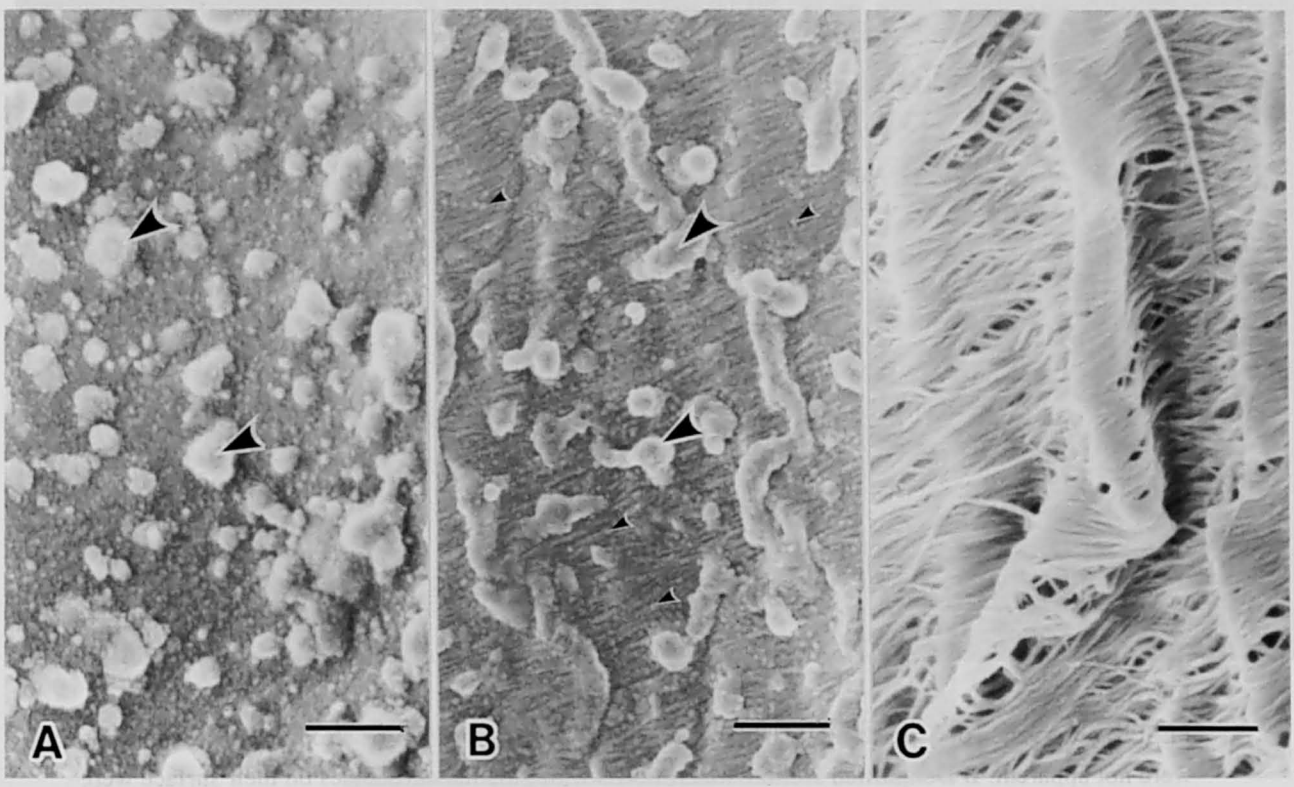

Fig. 5.2

FESEM observation of the innermost surface of a mature fiber. **A** Control section. Macrofibrils were not apparent. The surface was covered by a warty layer. **B** Delignified section. Macrofibrils with globular substances were visible, and warts remained. **C** Delignified and xylanase-treated section. Macrofibrils were visible and there were no globular substances. Macrofibrils were wavy due to extraction of large amounts of lignin and xylan. No warts were visible. Small arrowheads indicate globular substances (xylan) and large arrowheads indicate warts. Bars = 200 nm.

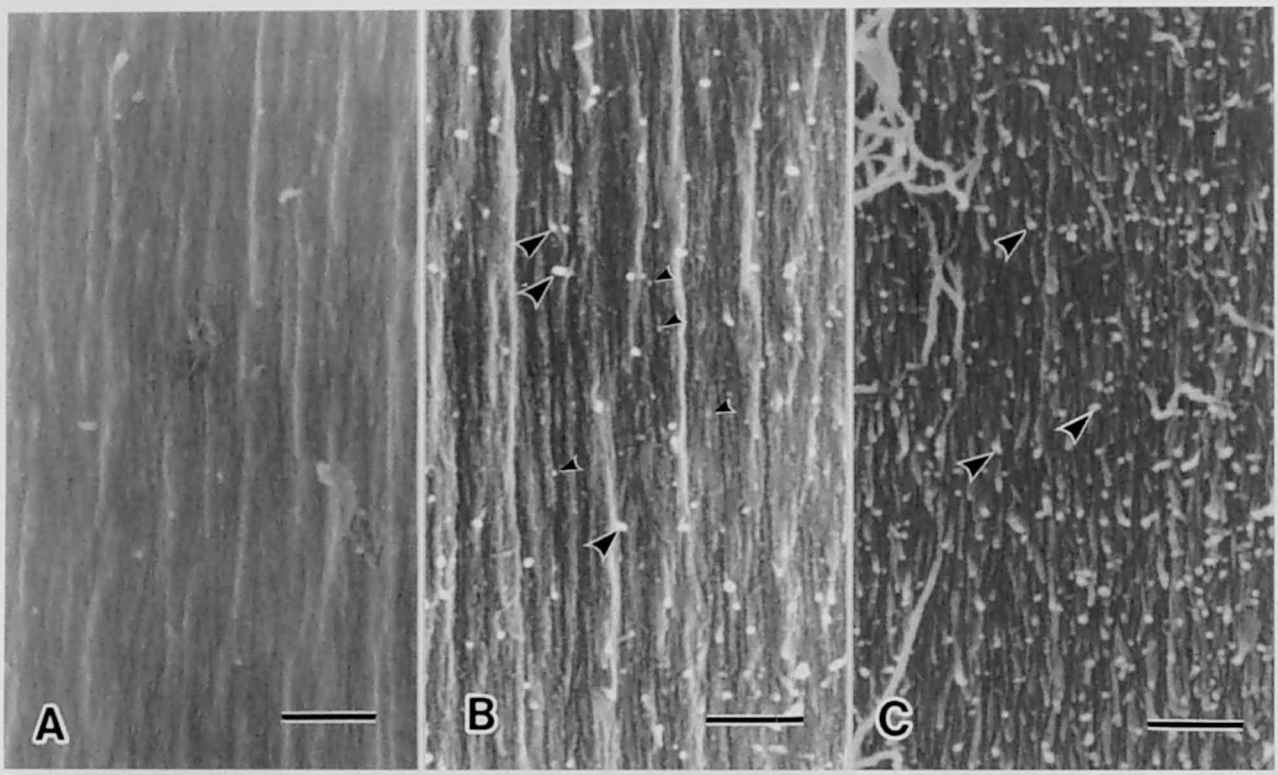

Fig. 5.3

FESEM observation of a sliced surface of the mature fiber secondary wall. **A** Control section. Macrofibrils were not apparent. **B** Delignified section. Macrofibrils with globular substances on their surface were visible. **C** Delignified and xylanase-treated sections. Macrofibrils were visible and had a smooth surface. Small arrowheads indicate globular substances (xylan). Large arrowheads indicate the end of a macrofibril. Bars = 200 nm.

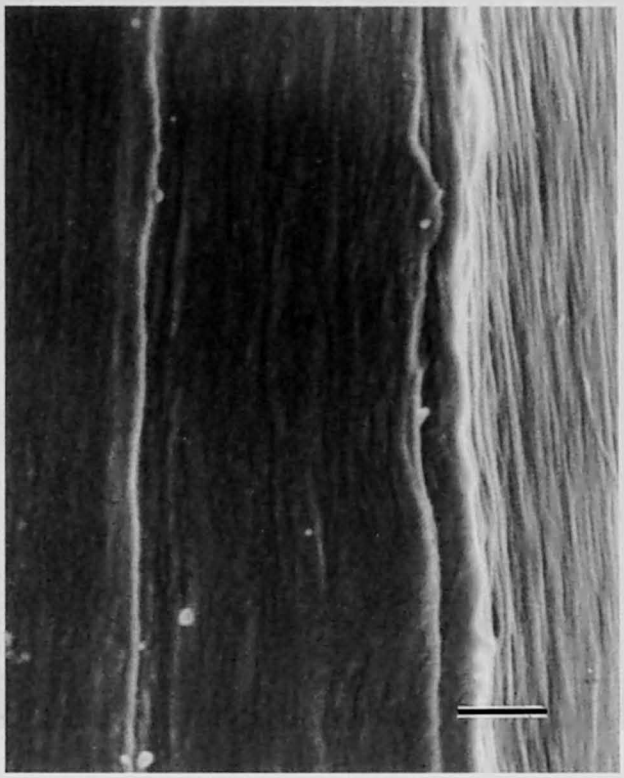

Fig. 5.4

FESEM observation of the sliced surface of an S_2-forming fiber secondary wall. Control section. Macrofibrils were apparent in the innermost surface (right) but were gradually indiscernible toward the outer part of the secondary wall (left). Bar = 200 nm.

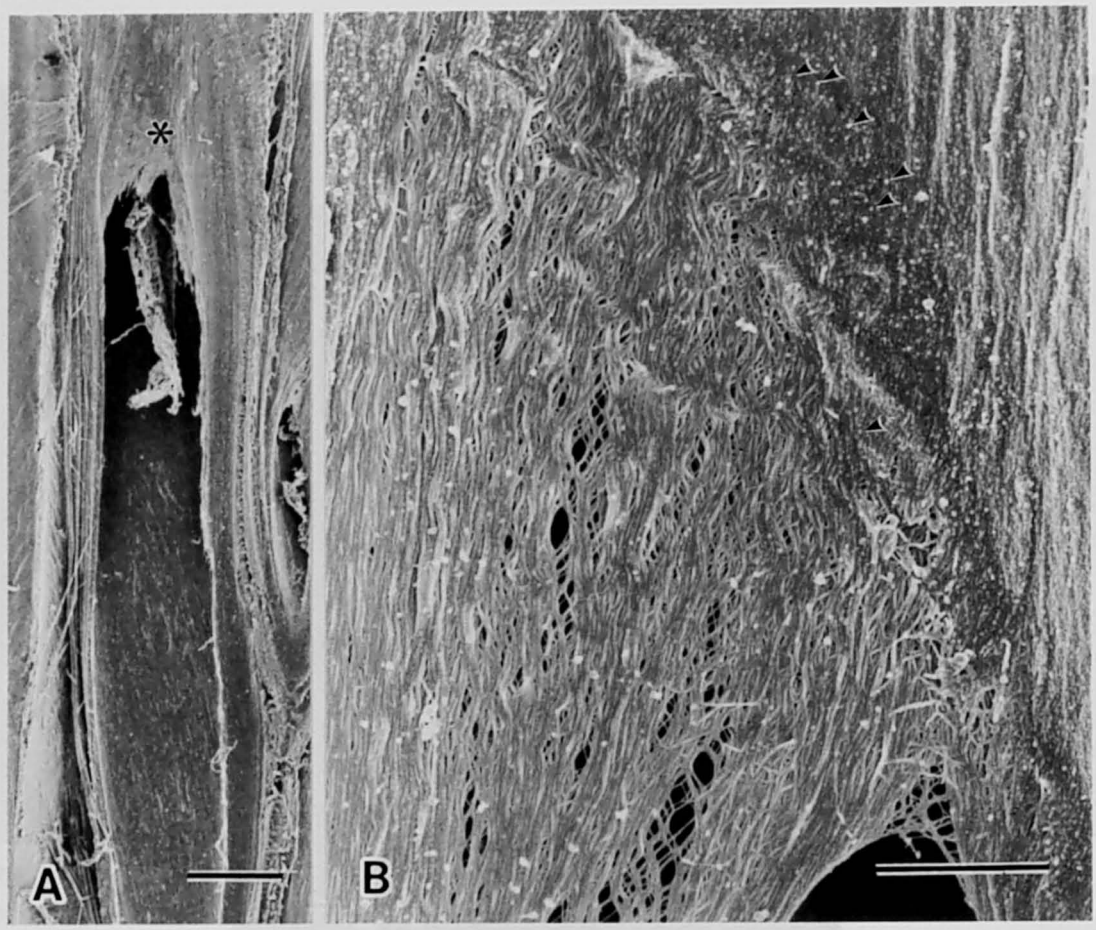

Fig. 5.5

FESEM observation of an obliquely sliced surface of the S_2-forming fiber secondary wall. Delignified section. **A** Overview of an S_2-forming fiber. Obliquely-sliced region (*) shows various stages of cell wall formation. Bar = 5 μm. **B** Detail of an obliquely-sliced differentiating secondary wall. Macrofibrils in the inner part had a smooth surface (left), but those in the outer part had globular substances on their surface (right). The globular substances gradually increased toward the outer part of the secondary wall. Small arrowheads indicate globular substances (xylan). Bar = 1 μm.

Chapter 6

Conclusion

The localization of xylan in differentiating xylem of *Fagus crenata* was observed by immunogold labeling. Anti-xylan antiserum was prepared and characterized. The antiserum could bind specifically to β-1,4-D-xylose moiety of xylan but not to other polysaccharides. Immunogold labeling was observed only in the secondary wall of xylem cells, i.e. vessel elements, wood fibers, axial parenchyma and ray parenchyma, but was not found in the compound middle lamella, pit chambers or cell lumen of these cells. The cell walls in the cambial zone and cell expansion zone were not labeled. At a subcellular level, the labeling of xylan was observed only in the secondary walls of xylem cells, but not in the primary walls and the middle lamella. Xylan was evenly distributed in the secondary walls except for the outer part of the S_1 layer in which it was less abundant. The labeling density in each secondary wall layer (S_1, S_2 and S_3) increased in the course of the cell wall formation. This result suggests that the deposition of xylan occurs in a penetrative way.

To reveal where xylan deposits within secondary wall and how xylan affects cell wall ultrastructure, especially fibril structure, immuno scanning electron microscopy with anti-xylan antiserum was applied. In S_1-forming fibers, fibrils were small in diameter and deposited sparsely on the inner surface of the cell wall. Fibrils with approximately 5 nm width (microfibrils) aggregated and formed thick fibrils with 12 nm width (macrofibrils). Some of these macrofibrils, which labeled positively for xylan, further aggregated to form bundles. In S_2-forming fibers, macrofibrils were thicker than those found in S_1-forming fibers and were densely deposited. Compared with newly formed secondary walls, previously formed secondary walls were composed of thick and highly packed macrofibrils. Labels against xylan were much more prevalent on mature secondary walls than on newly deposited secondary walls. This result implies that the deposition of xylan into the cell wall may occur continuously after macrofibril deposition and may be responsible for the increase in diameter of the macrofibrils.

The localization of xylan in *Fagus crenata* fiber was confirmed by selective extraction

with mild delignification and xylanase degradation. The data of chemical analysis suggested that sections were delignified with low loss of carbohydrates and xylanase selectively degraded xylan. Extraction occurred throughout 100 μm thick radial sections, shown by micrographs taken of the fiber cell wall located in the middle of thick sections. Immunogold labeling by anti-xylan antiserum was not observed in the xylanase-degraded sections while that was observed in the secondary wall of controls and delignified sections. The results support that xylan localized exclusively in the secondary wall. Xylanase degradation caused extensive swelling of the secondary wall. The secondary wall swelling might be due to the release of compressive stresses caused by the selective removal of xylan, suggesting that xylan might act as a cementing material for the lamellated structure of cellulose microfibrils in the secondary wall.

Ultrastructure of delignified and/or xylanase-treated secondary walls of *Fagus crenata* fibers were examined by FESEM. Macrofibrils with a smooth surface were visible in the innermost surface of the differentiating fiber secondary wall. There was no ultrastructural difference between control and delignified sections, indicating that lignin deposition had not started in the innermost surface of the cell wall. There was no ultrastructural difference between control and xylanase-treated sections. Macrofibrils on the outer part of the differentiating secondary wall had globular substances in delignified sections. These globular substances disappeared following xylanase treatment, indicating that these globules are xylan. The globular substances were not visible near the inner part of the differentiating secondary wall but gradually increased toward the outer part of the secondary wall, indicating that xylan penetrated into the cell wall and continuously accumulated on the macrofibrils. Mature fiber secondary walls were also examined by FESEM. Any fibrils were not apparent in the secondary wall in control specimens. Macrofibrils with many globular substances were observed in the delignified specimens. Following xylanase treatment, the macrofibrils had a smooth surface without any globules, indicating that the globular substance is xylan.

These results suggest that macrofibrils on the innermost surface of the secondary wall are coated with a thin layer of xylan and successive deposition of xylan into the cell wall increases macrofibril diameter. The large amounts of xylan that accumulated on macrofibrils appear globular, but are covered with lignin after they are deposited.

From the findings mentioned above, the following mechanism for xylan deposition and secondary wall assembly are proposed. There are two phases of xylan deposition. First, xylan coats the surface of macrofibrils that have just been released into the innermost surface of the cell wall. This thin layer of xylan could not be resolved by FESEM, but was immunolabelied with anti-xylan antiserum. Xylan, however, would not unite microfibrils into a macrofibril because microfibrils were not observed after xylanase degradation. Second, large amount of xylan penetrate into the cell wall because there is no room for xylan to coat the macrofibril surface. This type of xylan accumulates on the macrofibrils and has a globular appearance. Xylan might act as a cementing material for the lamellated structure of cellulose microfibrils in the secondary wall.

References

Abe H., Ohtani J., Fukazawa K. (1991) FE-SEM observation on the microfibrillar orientation in the secondary wall of tracheids. IAWA Bulletin, N.S. 12: 431-438

Abe H., Ohtani J., Fukazawa K. (1992) Microfibrillar Orientation of The Innermost Surface of Conifer Tracheid Walls. IAWA Bulletin, N.S. 13: 411-417

Awano T., Takabe K., Fujita M. (1998) Localization of glucuronoxylans in Japanese beech visualized by immunogold labelling. Protoplasma 202: 213-222.

Awano T., Takabe K., Fujita M., Daniel G. (2000) Deposition and localization of glucuronoxylans in the secondary cell wall of Japanese beech as observed using immuno FE-SEM. Protoplasma 212: 72-79

Awano T., Takabe K., Fujita M. (2002) Xylan deposition on the secondary wall of the *Fagus crenata* fiber. Protoplasma: *in press.*

Bastawde K. B. (1992) Xylan structure, microbial xylanases, and their mode of action. World Journal of Microbiology and Biotechnology 8: 353-368

Baydoun E. A. H., Brett C. T. (1997) Distribution of xylosyltransferases and glucuronyltransferase within the Golgi apparatus in etiolated pea (*Pisum sativum* L.) epicotyls. Journal of Experimental Botany 48: 1209-1214

Brett C. T., Healy S. A. , McDonald M. S., Macgregor C., Baydoun E. A. H. (1997) Binding of nascent glucuronoxylan to the cell walls of pea seedlings. International Journal of Biological Macromolecules 21: 169-173

Catesson A. M. (1983) A cytochemical investigation of the lateral walls of Dianthus vessels. Differentiation and pit-membrane formation. IAWA Bulletin. 4: 89-101

Catesson A. M., Funada R., Robert-Baby D., Quinet-Szely M., Chu-Ba J., Goldberg R. (1994) Biochemical and cytochemical cell wall changes across the cambial zone. IAWA Journal 15: 91-101

Cotê W. A., JR., Day, A. C., Timell, T. E. (1969) A contribution to the ultrastructure of tension wood fibers. Wood Science and Technology 3: 257-271

Delmer D. P., Amor Y. (1995) Cellulose biosynthesis. The Plant Cell 7: 987-1000

Donaldson L. A., Singh A. P. (1998) Bridge-like structures between cellulose microfibrils in radiata pine (Pinus radiata D.Don) kraft pulp and holocellulose. Holzforschung 52: 449-454

Effland M. (1977) Modified procedure to determine acid-insoluble lignin in wood and pulp. Tappi 60: 143-144

Fengel D. (1970) Ultrastructural behavior of cell wall polysaccharides. Tappi 53: 497-503

Fengel D., Wegener G. (1989) Wood. Chemistry, Ultrastructure, Reactions. Berlin: Walter de Gruyter.

Frey-Wyssling A. (1954) The fine structure of cellulose microfibrils. Science 119: 80-82

Fujino T., Itoh T. (1998) Changes in the three dimensional architecture of the cell wall during lignification of xylem cells in Eucalyptus tereticornis. Holzforschung 52: 111-116

Hafrén J., Fujino T., Itoh T. (1999) Changes in Cell Wall Architecture of Differentiating Tracheids of Pinus thunbergii during Lignification. Plant and Cell Physiology. 40: 532-541

Harada H. (1962) Electron microscopy of ultrathin section of beech wood (*Fagus Crenata* BLUME). Mokuzai Gakkaishi 8: 252-259

Harada H. (1965) Ultrastructure and organization of gymnosperm cell walls. In: Cellular ultrastructure of Woody Plants (Cotê, W. A., Jr., ed.), pp. 215-233. Syracuse Univ. Press.

Heyn, A. N. J. (1966) The microcrystaline structure of cellulose in cell walls of cotton, ramie, and jute fibers as revealed by negative staining of sections. Journal of Cell Biology. 29: 181-197

Heyn, A. N. J. (1969) The elementary fibril and supermolecular structure of cellulose in soft wood fiber. Journal of Ultrastructural Research. 26: 52-68

Itoh T., Ogawa T. (1993) Molecular architecture of the cell wall of poplar cells in suspension culture, as reveraled by rapid-freezing and deep-etching techniques. Plant and Cell Physiology 34: 1187-1196

Kataoka Y., Saiki H., Fujita M. (1992) Arrangement and superimposition of cellulose microfibrils in the secondary walls of coniferous tracheids. Mokuzai Gakkaishi 38: 327-335

Kerr A. J., Goring D. A. I. (1975) The ultrastructural arrangement of the wood cell wall. Cellulose Chemistry and Technology 9: 563-573

Klaudiz W. (1957) Zur biologisch-mechanischen Wirkung der Cellulose und Hemicellulose in Festigungsgewebe der Laudholzer. Holzforschung 11: 110-116

Labavich J. M., Ray P. M., 1974: Turnover of cell wall polysaccharides in elongating pea stem segments. Plant Physiology. **53**, 669-673

Maeda Y., Awano T., Takabe K., Fujita M. (2000) Immunolocalization of glucomannans in the cell wall of differntiating tracheids in *Chamaecyparis obtusa.* Protoplasma 213: 148-156

Maekawa E., Koshijima T. (1983) Evaluation of the acid-chlorite method for the determination of wood holocellulose. Mokuzai Gakkaishi 29: 702-707

Maekawa E., Ichizawa T., Koshijima T. (1989) An evaluation of the acid-soluble lignin determination in

analyses of lignin by the sulfuric acid method. Journal of Wood Chemistry and Technology 9: 549-567

McCann M. C., Roberts K. (1991) Architecture of the primary cell wall. In : The Cytoskeletal Basis of Plant Growth and Form. Edited by Lloyd, C.W. pp. 109-129. Academic Press, San Diego.

McCann M. C., Roberts K. (1994) Change in cell wall architecture during cell elongation. Journal of Experimental Botany. 45: 1683-1691

McNeil M., Albersheim P., Taiz L., Jones R. (1975) The structure of plant cell walls. VII. Barley aleurone cells. Plant Physiol. 55: 64-68

Meier H. (1961) The distribution of polysaccharides in wood fibers. Journal of Polymer Science 51: 11-18

Meier H., Wilkie K. C. B. (1959) The distribution of polysaccharides in the cell wall of tracheids of pine (Pinus silvestris L.). Holzforschung 13: 177-182

Migné C., Prensier G., Grenet E. (1994) Immunogold labelling of xylans and arabinoxylan the plant cell walls of maize stem. Biology of the Cell 81: 267-276

Mora F., Ruel K., Camtat J., Joseleau J. P. (1986) Aspect of native and redeposited xylans at the surface of cellulose microfibrils. Holzforschung 40: 85-91

Mühlethaler K. (1965) The Fine Structure of the Cellulose Microfibril. In: Cellular Ultrastructure of Woody Plants (Cotê, W. A., JR., ed.). Syracuse University Press, Syracuse, N. Y., pp. 191-198

Nakashima J., Mizuno T., Takabe K., Fujita M., Saiki H. (1997) Direct visualization of lignifying secondary wall thickenings in *Zinnia elegans* cells in culture. Plant and Cell Physiology 38: 818-827

Neville A. C. (1988) A pipe-cleaner molecular model for morphogenesis of helicoidal plant cell walls based on hemicellulose complexity. Journal of Theoretical Biology 131: 243-254

Northcote D., Davey R., Lay J. (1989) Use of antisera to localize callose, xylan and arabinogalactan in the cell-plate, primary and secondary walls of plant cells. Planta 178: 353-366

Osawa T., Yoshida Y., Tsuzuku F., Nozaka M., Takashio M., Nozaka Y. (1999) The advantage of the osumium conductive metal coating for the detection of the colloidal gold-conjugated antibody by SEM. Journal of Electron Microscopy 48: 665-669

Osumi M., Yamada N., Kobori H., Yaguchi H. (1992) Observation of colloidal gold particles on the surface of yeast protoplasts with UHR-LVSEM. Journal of Electron Microscopy 41: 392-396

Parameswaran N., Liese W. (1982) Ultrastructural localization of wall components in wood cells. Holz Roh- und Werkstoff 40: 145-155

Parameswaran N., Sinner M. (1979) Topochemical studies on the wall of beech bark sclereids by enzymic and acidic degradation. Protoplasma 101: 197-215

Pawley J. (1997) The development of field-emission scanning electron microscopy for imaging biological surfaces. Scanning 19: 324-336

Reis D., Roland J. C., Mosiniak M., Darzens D., Vian B. (1992) The sustained and warped helicoidal pattern of a xylan-cellulose composite: the stony endocarp model. Protoplasma 166: 21-34

Roland J. C., Mosiniak M. (1982) On the twisting pattern, texture and layering of the secondary cell walls of lime wood. Proposal of an unifying model. IAWA Bulletin 4: 15-26

Roy R., Katzenellenbogen E., Jennings, H. J.(1984) Improved procedures for the conjugation of oligosaccharides to protein by reductive amination. Canadian Journal of Biochemistry and Cell Biology 62: 270-275

Ruel K., Barnoud F., Goring D. A. I. (1978) Lamellation in the S2 layer of softwood tracheids as demonstrated by scanning transmission electron microscopy. Wood Science and Technology 12: 287-291

Satiat-Jeunemaitre B., Martin B., Hawes C. (1992) Plant cell wall architecture is revealed by rapid-freezing and deep etching. Protoplasma 167: 33-42

Sell J., Zimmerman T. (1993a) Radial fibril agglomerations of the S2 on transverse-fracture surfaces of tracheids of tension-loaded spruce and white fir. Holz als Roh- und Werkstoff 51: 384

Sell J., Zimmerman T. (1993b) The structure of the cell wall layer S2. Field-emission SEM studies on transverse-fracture surfaces of the wood of spruce and white fir. Forschungs und Arbeitsberichte EMPA Abteilung Holz 28: 1-26

Suzuki K., Ingold E., Sugiyama M., Komamine A. (1991) Xylan synthase activity in isolated mesophyll cells of *Zinnia elegans* during diffentiation to tracheary elements. Plant Cell Physiology 32: 303-306

Suzuki H., Kaneko T., Sakamoto T., Nakagawa M., Miyamoto T., Yamada M., Tanoue K. (1994) Redistribution of α-granule membrane glycoprotein IIb/IIIa (Integrin αIIIbβ3) to the surface membrane of human platelets during the release reaction. Journal of Electron Microscopy 43: 282-289

Suzuki K., Baba K., Itoh T., Sone Y. (1998) Localization of the xyloglucan in cell walls in a suspension culture of tobacco by rapid-freezing and deep-etching techniques coupled with immunogold labelling. Plant and Cell Physiology 39: 1003-1009

Suzuki K., Kitamura S., Kato Y., Itoh T. (2000) Highly substituted glucuronoarabinoxylans (hsGAXs) and low-branched xylans show a distinct localization pattern in the tissues of *Zea mays* L. Plant and Cell Physiology 41: 948–959

Takabe K., Fujita M., Harada H., Saiki H. (1981) The deposition of cell wall components in differentiating tracheids of Sugi. (in Japanese) Mokuzaigakkaishi 27: 249-255

Takabe K., Fujita M., Harada H., Saiki H. (1983) Changes in the composition and the absolute amount of sugars with the development of *Cryptomeria* tracheids. Mokuzaigakkaishi 29: 183-189

Takata K., Akimoto Y. (1988) Colloidal gold label observed with a high resolution backscattered electron imaging in mouse lymphocytes. Journal of Electron Microscopy **37**: 346-350

Taylor J. G., Haigler C. H. (1993) Patterned secondary cell-wall assembly in tracheary elements occurs in a self-perpetuating cascade. Acta Botanica Neerlandica 42: 153-163

Terashima N., Fukushima K, He L. F., Takabe K. (1993) Comprehensive model of the lignified plant cell wall. In: Forage Cell Wall Structure and Digestibility. (Jung, H.G., Buxton, D.R., Hatfield, R.D., Ralph, J., eds.)

Vian B. (1982) Organized microfibril assembly in higher plant cells. In: Cellulose and other natural polymer systems. Brown R. M., ed. Plenum. New York. pp.23-43

Vian B., Brillouet J., Satiat-Jeunemaitre B. (1983) Ultrastructural visualization of xylans in cell walls of hardwood by means of xylanase-gold complex. Biology of the Cell 49: 179-182

Vian B., Reis D., Mosiniak M., Roland J. C. (1986) The glucuronoxylans and the helicoidal shift in cellulose microfibrils in linden wood: Cytochemistry in muro and on isolated molecules. Protoplasma 131: 185-199

Vian B., Roland J. C., Reis D., Mosiniak M. (1992) Distribution and Possible Morphogenetic Role of The Xylans within the Secondary Vessel Wall of Linden Wood. IAWA Bulletin, n. s. 13: 269-282

Vian B., Reis D., Darzens D., Roland J. C. (1994) Cholesteric-like crystal analogs in glucuronoxylan-rich cell wall composites : experimental approach of acellular re-assembly from native cellulose. Protoplasma 180: 70-81

Wise L., Murphy M., Addieco A. (1946) Chlorite holocellulose, its fractionation and bearing on summative wood analysis and on studies on the hemicelluloses. Paper Trade Journal 122: 35-43

Yoshida M., Hosoo Y., Okuyama T. (2000) Periodicity as a factor in the generation of isotropic compressive growth stress between microfibrils in cell wall formation during a twenty-four hour period. Holzforschung 54: 469-473